

Article

Passive Energy-Saving Optimal Design for Rural Residences of Hanzhong Region in Northwest China Based on Performance Simulation and Optimization Algorithm

Teng Shao ^{1,*} , Wuxing Zheng ¹ and Zheng Cheng ²

¹ School of Mechanics, Civil Engineering and Architecture, Northwestern Polytechnical University, Xi'an 710072, China; wxzheng@nwpu.edu.cn

² College of Pipeline and Civil Engineering, China University of Petroleum, Qingdao 266580, China; Qingqingczcz@163.com

* Correspondence: shaoteng@nwpu.edu.cn

Abstract: The rural residences of Northwest China are characterized by a state of high energy consumption and low comfort due to the limited economic level and awareness of energy-saving compared with the urban residences. To remedy this, appropriate passive design strategies should be adopted first, in order to provide a design mode with low energy consumption and low cost for rural residences under the premise of thermal comfort. In this paper, taking Hanzhong region (Shaanxi Province, China) as an example, we establish a benchmark model based on a field survey and develop an optimization process by combining EnergyPlus simulation software, the MOBO optimization engine, and weighted sum method. The action mechanisms of passive design parameters, including the building orientation, length–width ratio, building envelope parameters, external shading system, and window–wall ratio, on heating, cooling, and total energy consumption are analyzed, and the quantitative relationships between single-parameter and energy consumption are established. Then, the mutually restricted indices of total energy consumption and initial investment cost are taken as optimization objectives, and 17 design parameters are selected as the optimization variables. The NSGA-II algorithm is adopted to conduct the multi-parameter, multi-objective optimization design for rural houses in Hanzhong area, through coupling of the EnergyPlus and MOBO software. In this way, Pareto solutions are obtained and the value distributions of the multi-objectives and design parameters are analyzed. Based on the actual requirements of decision-makers and using the weight method, three design schemes focusing on different performance tendencies are proposed. The results indicate that by using the proposed optimization process, the building energy consumption can be significantly reduced while taking initial investment costs into account, where the energy-saving rate is in the range of 31.9–61.5%. When the EC/IC ratio is 1:1, 2:1, and 1:2, the energy-saving rate can reach 51.5%, 57.8%, and 43.5%, respectively. It can provide a beneficial pattern for the energy-saving design and renovation of rural residences in Hanzhong area of China.

Keywords: rural residence; passive energy-saving design; building energy consumption; performance simulation; multi-objective optimization



Citation: Shao, T.; Zheng, W.; Cheng, Z. Passive Energy-Saving Optimal Design for Rural Residences of Hanzhong Region in Northwest China Based on Performance Simulation and Optimization Algorithm. *Buildings* **2021**, *11*, 421. <https://doi.org/10.3390/buildings11090421>

Academic Editor: Benedetto Nastasi

Received: 16 August 2021

Accepted: 17 September 2021

Published: 21 September 2021

Publisher's Note: MDPI stays neutral with regard to jurisdictional claims in published maps and institutional affiliations.



Copyright: © 2021 by the authors. Licensee MDPI, Basel, Switzerland. This article is an open access article distributed under the terms and conditions of the Creative Commons Attribution (CC BY) license (<https://creativecommons.org/licenses/by/4.0/>).

1. Introduction

Reducing the building energy consumption and carbon emission has become the focus of the international community due to high energy prices and climate change [1]. The carbon emissions generated during the whole life of buildings account for 30% of total global carbon emissions and will account for 50% by 2050 if they continue to grow at their present rate [2]. Thereby, many countries have proposed the solutions to improve the energy utilization level of buildings, such as promoting ultra-low energy or near zero energy buildings, and to reduce the influence of climate change. Energy saving design in buildings plays an important role in solving the energy and environmental problems

of China's construction industry; however, it is mostly focused on the urban buildings at present, while the rural areas of China are vast and spread across the country. The dwelling overall floorage was about 27.8 billion square meters, about 65% of the rural total building areas in China [3]. With the synchronous development of urban and rural regions in China, the demands of villagers for living environment have also been increasing. It is obviously different in built ways from urban residences, and most rural residences are self-built and self-financed according to the personal preference or traditional experience [4], while lacking consideration of building energy-saving design. However, most of the energy-saving standards are appropriate for the urban buildings in China. In 2019, the commodity and biomass energy consumption in the operating process of rural houses reached 222 million and 90 million tons of standard coal, respectively, including that used for heating, cooling, cooking, lighting, and so on, with a proportion of 28.1% for the total energy consumption of civil buildings [5]. "Actively promote energy conservation in rural housings" became one of the major tasks considered by the Chinese government in 2017 [6].

Building energy saving design should be conducted in accordance with the local climatic, resource, and economic conditions [7]. It mainly includes active design and passive design. Active design refers to the use of building equipment to maintain comfortable indoor environment, such as heating, air condition, ventilation, and so on. Passive design is the opposite concept, where the indoor environment is improved and the building energy consumption is reduced through the rational building design [8]. It accounts for a considerable proportion for the green building evaluation. In China, the passive energy saving design for rural residences has attracted many scholars to carry out a research because of the unique regional climate and environment, for example, rammed earth houses in Southern Shaanxi [9], cave-dwellings in the Loess Plateau [10], waterside dwellings in the Lower Yangtze Basin [11], herdsman houses in Qinghai Province [12], rural houses in Sichuan [13] and Lhasa [14], vernacular houses in Northern Hebei Province [15], Tibetan traditional dwellings in the cold region of Gannan [16], swallow dwellings in Western Hunan [17], yurts in the Mongolian grassland [18], rural houses in severely cold regions of northeast China [19–21], and so on. The passive design strategies adopted mainly include building layout and orientation, spatial scale and layout, building envelope, regional materials, sun-space and shading measures, and so on, where some studies have only focused on certain aspects. Due to the differences in geographic and climatic characteristics, although the same design strategy is adopted, the effects on building energy consumption and indoor thermal environment are not the same in different areas. In addition, most of the studies have aimed at the integrated application and effect evaluation of design strategies. As such, the quantitative analysis of passive energy-saving design is rare; that is, explore the quantitative relationships between passive technical parameters and building energy consumption. More importantly, compared with cities, the low level of the rural economy, as a key factor, affects the implementation of energy-saving technology. Existing studies usually focus on whether to meet the demands of energy-saving design standards, but lag behind in terms of economic considerations. On the one hand, the cost is considered from the view of the life cycle, such as Li [22] analyzed the effects of different energy saving measures adopted by rural houses in cold and severely cold regions, and obtained the building envelope parameters with the lowest cost over the life cycle. On the other hand, it is analyzed from the view of investment payback period after the design strategy is applied; for example, Lv [23] analyzed the relationships between design parameters and energy consumption of rural dwellings in Quanzhou, Fujian Province, obtained the combination of design parameters to minimize the energy consumption, and calculated the corresponding investment payback period. These studies lacked consideration of the synergistic effect between energy consumption and investment costs at the early design stage, and the results are not conducive for architects to make design decisions in advance. Therefore, determining a set of passive design measures that can minimize the building energy consumption and the related costs becomes an important means to realize the energy saving for rural houses.

Moreover, building energy conservation and costs are affected by the synthetic action of passive design parameters, where the influencing mechanism of each parameter on the energy consumption is not isolated, such that coupling and interaction should be considered. It is unable to easily decide whether each parameter combination achieves better effect by the conventional design method. For solving the contradiction between two different performance indices under the control of various parameters in the design, many studies have been carried out by adopting crossover methods, such as machine learning, optimization algorithm, performance simulation, and so on. For example, studies have focused on the trade-off between building energy consumption and indoor thermal comfort [24–27], and the analysis of synergistic energy consumption and cost [28,29]. Furthermore, some studies have aimed at three or more objectives, such as Zhu et al. [30], who used a multi-objective optimization module in Grasshopper to optimize the energy consumption, PPD, and daylighting performance for three types of rural tourism building in northern China. Hong et al. [31], considering a library facility in a monsoon climate, took the PMV, initial investment cost, energy consumption, net present value and global warming potential as objectives, and adopted the EnergyPlus software and NSGA-II to conduct optimization.

In summary, a typical rural house, located in Hanzhong, Shaanxi, a region characterized by hot summer and cold winter, is selected as an example, and this article aims: (1) To systematically analyze the quantitative relationships between passive design parameters and building energy consumption, and reveal the influence mechanism; and (2) to obtain the combination of passive design parameters that can optimize building energy consumption and initial investment cost synergistically, thus providing help for the decision-making of energy saving design in the stage of scheme design.

2. Methods

2.1. Field Survey

By the means of field survey and analysis, we can determine the current situation of typical rural residences in Hanzhong, such as building form, building envelope's thermal performance, indoor thermal comfort level, energy use, and so on, to provide the basis for this study. In this paper, the typical villages in Hanzhong were selected to conduct a field survey and test, for a total of 200 questionnaires. According to the construction time, rural houses can be divided into traditional and modern forms. Traditional houses are mostly single-storey buildings, with three parts and single depth. Rammed earth or stone are used for the external wall. The 2.5 m overhang eaves and small windows are conducive to shading, but lead to a poor lighting effect. Traditional houses are gradually unable to meet the living needs of rural residents, and most of them are only used for storage or temporary use, with residents turning to modern houses. Although the newly built houses inherit some ecological experience of traditional dwellings, there are also some problems as follows:

Building form—typical forms of modern rural houses in Hanzhong are shown in Figure 1. Most modern houses (about 70%) are two- or three-storey brick structure buildings, with a building area of 100–200 m². The roof form is dominated by sloped roofs. Compared with traditional houses, the window area is obviously enlarged, with better lighting effect. However, the exterior window has both positive and negative effects on building energy consumption; additionally, the lack of shading measures is not conducive to heat prevention in summer.

Building envelope—it has poor thermal performance and fails to acclimatization. For example, 240 mm brick walls are commonly used for external walls, with a heat transfer coefficient of 1.96 W/m²·K. The roof is made of reinforced concrete board, without insulation measures, and the inner surface temperature can easily become too high in summer. External windows are mostly single-layer wooden or aluminum windows (accounting for about 60%), with a heat transfer coefficient of 5.80 W/m²·K. Double-layer aluminum windows only account for 30%, and few have adopted plastic-steel windows. These are

the main factors that affect the energy consumption and indoor thermal environment of rural houses.



Figure 1. Typical forms of modern rural houses in Hanzhong [32].

Thermal comfort—the survey results on thermal comfort are shown in Figure 2. In terms of thermal sensation voting (TSV), with the scale of “−3—cold, −2—colder, −1—slightly cold, 0—moderate, +1—slightly hot, +2—hotter, +3—hot”, 65% of residents felt hot (TSV = +1–+3) in summer and 63% felt cold (TSV = −1–−3) in winter. Although clothing can have a regulatory effect on thermal comfort, from the perspective of thermal preference, with the scale of “1—rise, 2—remain unchanged, 3—decrease”, 79% of residents preferred lower temperature (+3) in summer and 88% preferred higher temperature (+1) in winter. These results indicate that residents hoped that their indoor thermal environment could be improved. It can be seen from the testing results that the average indoor temperature (January) was about 7.7 °C, significantly less than 14 °C in winter stipulated in the national standard of <Design standard for energy efficiency of rural residential buildings> [33]. The mean indoor temperature in summer (July) was about 28.6 °C and, so, some cooling measures are needed.

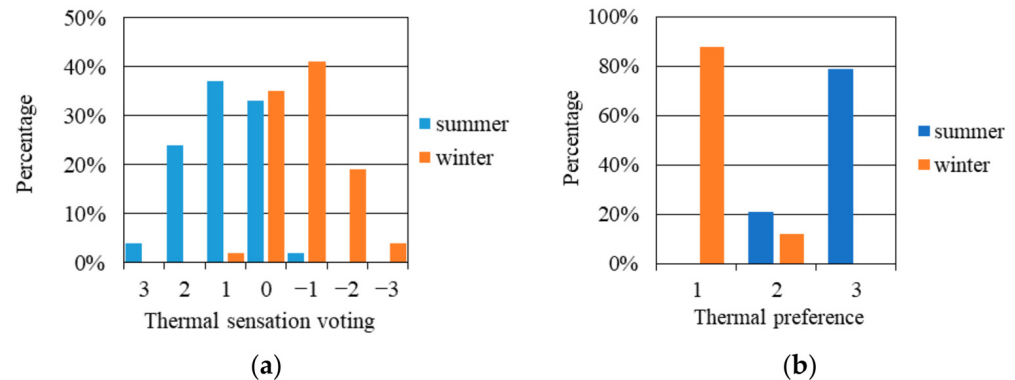


Figure 2. Survey results on thermal comfort: (a) thermal sensation voting; (b) thermal preference.

Energy use—the cooling equipment in summer is mainly air conditioners and electric fans, and the heating equipment in winter is mainly heating boiler, electric heaters, etc. Therefore, electricity and coal are the main energy sources for heating and cooling in this region. Firewood is used for auxiliary heating in winter, but coal is generally used from December to February. The usage amount varies, according to the family economic conditions: 14% of the families used less than 200 Kg of coal in winter, 49% used 200–400 kg, 15% used 400–800 kg, 10% used 800 kg–1000 kg, and 12% of families relied on burning firewood for heating in winter, with daily use of about 5 Kg. The energy consumption in the cooling period is about 3–4 times that in the transition season, while that in the heating period is about 5 times. Even so, the indoor thermal environment is still unsatisfactory for the comfort requirements, and it can only rely on increasing energy use.

Economic income—The number of permanent residents in a family was 2–5, and per capita disposable income ranged from ¥ 5000 to ¥ 6000. Such low income limits the investment in improving the building performance. Through the interviews, it was found that rural residents mainly considered the economy, safety, aesthetics, and so on, and

seldom paid attention to the issues about energy-saving, such as the building envelope's thermal performance, indoor thermal comfort, etc. This situation shares similarities with other low-income rural areas in China [4].

In summary, it can be seen that, due to the climatic conditions, economic level, and resident's awareness of energy conservation, coupled with the lack of professional design guidance, the local rural houses need to be improved, in terms of spatial shape, envelope structure, and shading system, among other factors.

2.2. Baseline Model

According to the survey results, one-storey residence has been gradually phased out in rural areas, and the two-storey house has become the main building form. Therefore, this study took two-storey house as the research object. According to the functional requirements, spatial layout and scale, and the living and production habits of rural residents, based on the field investigation, a benchmark model of rural houses in this region was built. It should be noted that this model is the energy space of the rural house, and the external styling or additional space can be designed according to the preferences of residents. The basic information is as follows: the building area is 200 m², consisting of living rooms, bedrooms, a dining room, a kitchen, a storeroom and toilets, which can meet the living needs of ordinary families. The heights of the first and second floor are 3.3 m and 3.0 m, respectively [32]. The floor plan is shown in Figure 3, and the house was modeled by using the EnergyPlus software.

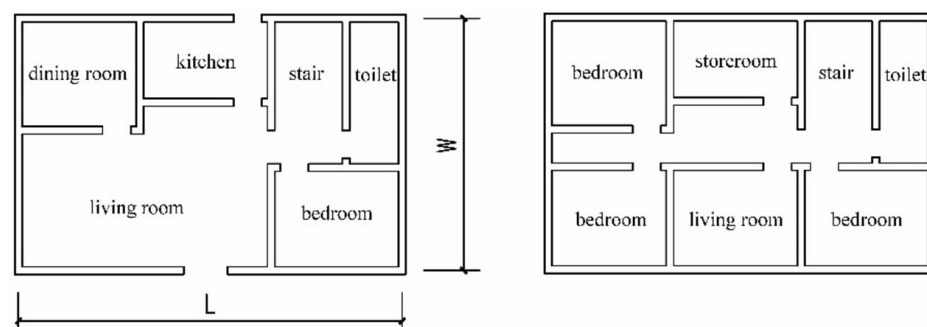


Figure 3. Floor plan of a typical rural house.

2.2.1. Meteorological Data

China is divided into five climate zones in accordance with the thermal design for civil buildings, including severely cold region, cold zone, hot summer and cold winter zone, hot summer and warm winter zone, and mild zone [34]. Hanzhong, located in southwest Shaanxi province, at a northern latitude of 33.07° and eastern longitude of 107.03°, is a hot summer and cold winter zone (defined as regions where the average temperature is between 0 °C and 10 °C in the coldest month and between 25 °C and 30 °C in the hottest month, with the number of days below the average temperature of 5 °C being between 0 and 90 days and above the average temperature of 25 °C being between 40 and 110 days). The Chinese Standard Weather Data (CSWD) of Hanzhong was selected as the outdoor calculation parameter for the simulation. As shown in Figure 4, the annual mean temperature is 14.6 °C, and the total annual solar radiation is 4196.7 MJ/m². In winter (from December to February), the daily mean temperature ranges from −0.11 °C to 7.28 °C, with a daily minimum temperature −4.8 °C. In summer (from June to August), the daily mean temperature varies in the range of 20.5 °C–29.8 °C, with a daily maximum temperature of 35.2 °C. Due to the climate difference between winter and summer, we should not focus on the heat preservation in winter, but also pay attention to heat protection in summer when designing rural houses.

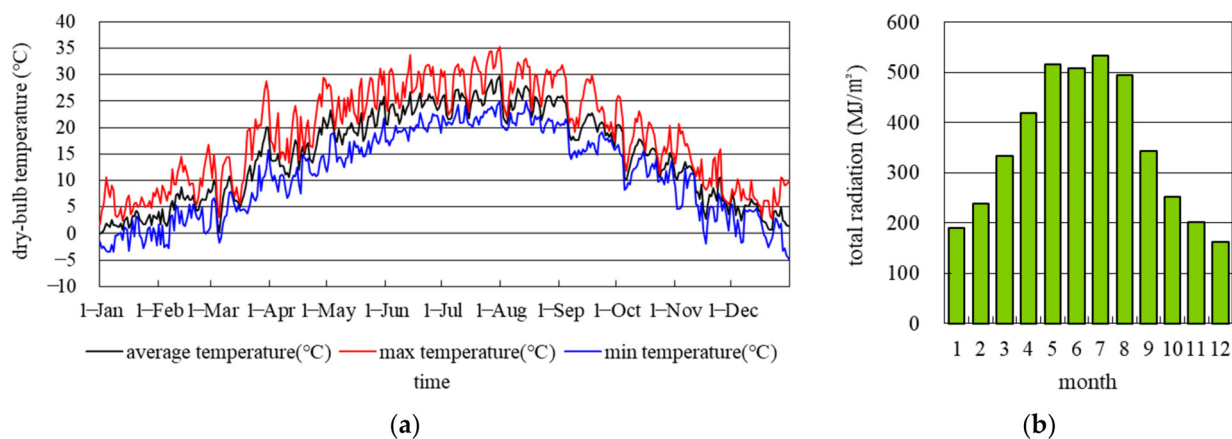


Figure 4. The typical year meteorological data of Hanzhong: (a) daily dry-bulb temperature; (b) monthly total solar radiation.

2.2.2. Parameters of Retained Building Envelope

Referring to the relevant stipulation of the <Design standard for energy efficiency of rural residential buildings> [33], and considering the field survey results and local materials, the building envelope's initial parameters are presented in Table 1. The load-bearing structure of external wall is 240 mm shale solid brick. The roof is made of "flat roof part + slope roof part", with the reinforced concrete slab in the flat roof and the form of "roof truss + tile" in slope roof. Detailed information of the building envelope is also provided in Table 1.

Table 1. Building envelope parameters for the benchmark model.

Parts	Construction
External wall	Exterior surface + 240 mm shale solid brick + 20 mm composite mortar
Roof	Tile + roof truss + 20 mm cement mortar + 100 mm reinforced concrete slab
Ground	Surface layer + damp-proof layer + 20 mm cement mortar + 100 mm fine aggregate concrete
External window	Single-frame single-glass aluminum window

2.2.3. Heating and Air Conditioning Systems

The paper mainly compares building energy consumption of different design schemes, in which the variables only include architectural ontology's design parameters. Therefore, the equipment parameters are set as the fixed and normalized values, to ensure the comparability of simulation results. Combining with the relevant provisions in the national standards <Design standard for energy efficiency of residential buildings in hot summer and cold winter zone> [35] and <Design standard for energy efficiency of rural residential buildings> [33], as well as the actual situation of rural houses in Hanzhong region, the relevant parameters of the heating and air condition systems were set as follows: (1) The heating and cooling setpoint temperatures are 14 °C and 26 °C, with an air change rate of 1.0 h⁻¹; (2) the heating period is from December 1 to February 28 of the next year, and the cooling time is from June 15 to August 31; and (3) the mean intensity of indoor heat gain is set as 4.3 W/m². The household heating boiler and split air conditioner were adopted, with the heat efficiency of 0.82 and energy efficiency ratio (EER) of 3.4. According to residents' living habits and usage requirements for each room, the air conditioners were only installed in living rooms and bedrooms on each floor. The operating schedule was set as follows: 12:00–14:00 and 21:00–08:00 turned on in bedrooms; for the living room, 18:00–21:00 on weekdays, and 08:00–12:00 and 14:00–21:00 on weekends. It can be obtained from the simulation that total energy consumption of benchmark model was 88.3 kW·h/m², including 64.7 kW·h/m² for heating energy consumption and 23.6 kW·h/m² for cooling energy consumption.

2.3. Optimization Platform: Coupling of EnergyPlus and MOBO

For solving the energy consumption, the simulation software can provide the help for building energy-saving design. EnergyPlus, a building energy simulation engine developed by the Department of Energy and Lawrence Berkeley National Laboratory, can be applied to the simulation of heating, cooling, lighting, and other energy consumption at any stage in the architectural design. Moreover, the software adopts the input and output mode of ASCII text format, allowing for easy communication and interface with other software. The simulation results of EnergyPlus were evaluated using the ANSI/ASHRAE standard 140-2007 [36]. Some studies about building energy consumption have been conducted using EnergyPlus [25,37]. EnergyPlus is used in this paper to explore the quantitative relationships between design parameters (including building form, building envelope and building interface) and energy consumption.

Multi-objective building optimization (MOBO), a universal free software product, can solve the problems of single- and multi-objective optimization, and also can be coupled with various other numerical simulation software, such as EnergyPlus, IDA-IEC, TRNSYS, etc. It can automatically change the parameters that need to be optimized and realize the iterative operation process. In addition, MOBO contains an optimization algorithm library, such as genetic algorithm, hybrid algorithm, Hooke-Jeeves algorithm, exhaustive algorithm, random algorithm, and so on, which has a strong applicability and handling capacity [38].

The non-dominated sorting genetic algorithm (NSGA-II), developed by Deb et al. (Deb et al. 2002), is one of the most popular and reliable multi-objective optimization algorithms which can be adopted for building performance optimization [39]. NSGA-II is a modified version of NSGA, and has the characteristics of better sorting algorithm, incorporates elitism, and no sharing parameter needs to be chosen. It also has the advantages of fast running speed and good convergence, and has become a benchmark for other multi-objective optimization algorithms. There have been many applications of NSGA-II [40–44]. Referring to relevant research and the hint of MOBO software [28,45], under the premise of ensuring result accuracy and reasonable calculation time, the parameter settings for NSGA-II were as follows: population size, 16; generation number, 126; crossover probability, 0.25; and mutation probability, 0.01. The process of optimization is halted once the maximum number of generations (equal to the generation number \times population size, i.e., 2016 iterations in this study) is reached.

Through coupling the EnergyPlus and MOBO software, the NSGA-II algorithm was adopted to study the multi-objective collaborative optimization. Thus, the cyclic calculation, identification, and judgment process of “performance simulation–result feedback–target determination” is realized, and the Pareto optimal solutions of design variables were obtained. The optimization process is depicted in Figure 5.

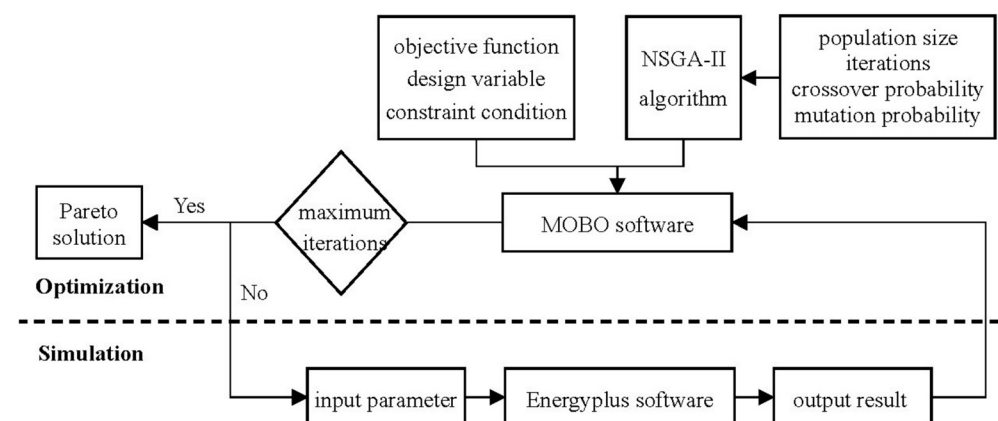


Figure 5. Optimization process by coupling EnergyPlus and MOBO software.

2.4. Multi-Attribute Decision Making

The method of multi-attribute decision-making is an important step in determining the design patterns. Pareto non-dominated solutions can be outputted using the optimization platform, and the design parameter combination of each solution can make the building energy consumption and initial investment cost synergistically optimized. However, in practical design, it is necessary to determine one or several groups of parameter combinations; thus, the multi-attribute decision-making method was required to deal with the Pareto solutions. This method involves solving the decision problem of selecting the optimum scheme or ranking scheme when considering multiple attributes (or objectives).

In decision theory, the weighted sum method (WSM) is a commonly used method. This method first determines the weight of each decision objective; which, in this study, were building energy consumption (EC) and initial investment cost (IC). Because of the different dimensions of each objective function, the data then need to be normalized. Thus, the weighted value of each solution (i.e., design scheme) can be obtained, which serves the basis for ordering each scheme. It can be calculated as follows:

$$F(x) = \sum_{i=1}^k W_i \times \frac{f_i(x) - f_i(x)^{\min}}{f_i(x)^{\max} - f_i(x)^{\min}} \quad (1)$$

where $F(x)$ is the weighted value (when its value is minimal, it is the optimal design scheme); $f_i(x)$ is the objective function value; $f_i(x)^{\max}$ and $f_i(x)^{\min}$ are the maximum and minimum values of each objective function; w_i is the weight coefficient of building energy consumption and initial investment cost, where the sum of weight coefficients is 1; and k represents the number of objective ($k = 2$ in this study).

2.5. Passive Design Parameters

The most important passive design parameters affecting the building energy consumption of rural dwellings in Hanzhong can be categorized into building form parameters, building envelope parameters, and building interface parameters. The specific parameters were set as follows.

2.5.1. Parameters of Building Form: Orientation and Building Shape

The building form parameters include building orientation and shape in this study. Solar radiation is one of the significant factors affecting the building energy consumption and indoor thermal environment, and has varying features for different orientations. Selecting an optimal orientation is the first consideration in the scheme design phase. The building shape is determined by the building length, width, and height, but the floor area is usually a fixed value, such that the adjustable range of ceiling height is small. Therefore, the length–width ratio was taken as an index to analyze the effect rule of building form on energy consumption. Table 2 shows the parameter settings for building orientation and length–width ratio.

Table 2. Parameters settings for building orientation and length–width ratio.

Parameter Name	Initial Value	Minimum Value	Maximum Value	Step Size
Building orientation	0° (south)	−90°	90°	5°
Length–width ratio	1.5	0.7	2.5	0.2

2.5.2. Parameters of Building Envelope: External Wall, Roof and Window

The building envelope's thermal performance directly restricts the energy consumption and indoor thermal environment, among which the parts in contact with the outdoor environment include external walls, roof, and windows.

- External wall

Thermal insulation for the exterior wall is a widely used energy-saving measure in rural houses. Due to its small size and independent type, the area of exterior wall accounts for a great part of building surface area, and the heat transfer consumption occupies about 40% of the whole building [46]. Table 3 shows the typical thermal insulation structure of exterior walls. The insulation material's type and thickness will affect its thermal performance, namely heat transfer coefficient. The physical properties of insulation materials can be seen in Table 4. The insulation material thickness was set in the range of 0–0.3 m, at a step size of 0.01 m in the simulation analysis.

Table 3. Typical thermal insulation structure of exterior wall for rural houses.

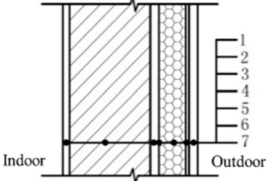
Name	Diagram	Layer
External thermal insulation of shale solid brick		1—20 mm composite mortar 2—240 mm shale solid brick 3—Screed-coat (cement plaster) 4—Cementing compound 5—Insulation layer 6—5 mm anti-crack mortar with alkali resistant glass fiber mesh cloth 7—Exterior surface

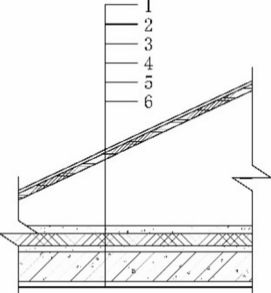
Table 4. Physical properties of insulation materials used in rural housing.

Parts	Name	Density (kg/m ³)	Heat Conductivity Coefficient (W/m·K)	Specific Heat (J/kg·K)
External wall, roof	Expanded polystyrene board (EPS)	15	0.040	1400
	Extruded polystyrene board (XPS)	35	0.030	1400
	Perlite board (PER)	120	0.070	1170
	Polyurethane board (PUR)	35	0.026	1590

- Roof

As shown in Table 5, for the mode of “slope roof + flat floor”, the insulation layer is usually set in the flat floor part. This saves the insulation material area and reduces the heat dissipation area of interior space, as well as increasing its integrity and aesthetics. The insulation material for a roof is same as that for the external wall, with the thickness also ranging from 0–0.3 m, and has a step size of 0.01 m in the simulation.

Table 5. Typical thermal insulation structure of roof for rural houses.

Name	Diagram	Layer
Reinforced concrete roof (waterproofing is undertaken by the slope roof)		1—Slope roof 2—Covering layer 3—Insulating layer 4—20 mm cement plaster 5—Reinforced concrete board 6—Interior surface

- External window

Compared with the non-transparent envelope, external windows, as transparent envelopes, are the weak places for thermal insulation, and also have great potential for

energy saving. The thermal performance of an external window is mainly determined by the heat transfer coefficient (K) and solar heat gain coefficient (SHGC). Twelve types of external windows were chosen for analysis, including two conditions: (1) with the same K-values and different SHGC-values (NO.3-NO.6); and (2) with the similar SHGC-values and different K-values (NO. 6-NO.9, NO.10-NO.12). The window type of NO.1 is commonly used in Hanzhong area at present. The external window types and parameters are shown in Table 6.

Table 6. External window types and parameters.

Number	Window Type	K (W/m ² ·K)	SHGC
1	Single clear 6 mm	5.778	0.819
2	Single Low-e clear 6 mm	3.779	0.720
3	6 mm clear + 6A + 6 mm grey	3.094	0.485
4	6 mm clear + 6A + 6 mm bronze	3.094	0.504
5	6 mm clear + 6A + 6 mm green	3.094	0.507
6	6 mm clear + 6A + 6 mm clear	3.094	0.700
7	6 mm clear + 9A + 6 mm clear	2.822	0.702
8	6 mm clear +12A + 6 mm clear	2.685	0.703
9	6 mm clear + 15A + 6 mm clear	2.665	0.703
10	6 mm clear + 6A + 6 mm Low-e	2.429	0.569
11	6 mm clear + 9A + 6 mm Low-e	1.977	0.568
12	6 mm clear + 12A + 6 mm Low-e	1.771	0.568

Note: Generic clear 6 mm—6 mm clear; Generic bronze 6 mm—6 mm bronze; Generic grey 6 mm—6 mm grey; Generic green 6 mm—6 mm green; Low emissivity 6 mm—6 mm Low-e; Air—A.

2.5.3. Parameters of Building Interface: Shading System and Window-Wall Ratio

- External sun-shading

If the building lacks an effective sun-shading device, excessive solar radiation will be introduced into the indoor space in summer, resulting in an increase in cooling energy consumption. External shading system can play this role for rural houses. The south side receives the most solar radiation, the east and west facades of rural houses are usually not equipped with exterior windows, and the effect of a north sun visor is small because of less solar radiation. So, the external shading system for south facing windows is mainly discussed in this paper, which has the form of a horizontal visor. The main parameters that affect the shaded effects include the overhang length of sunvisor (OL), the extension length of sunvisor (EL), the tilt angle of sunvisor (TA), and the distance between the sunvisor and the top edge of window (DSW), as shown in Table 7. Limited by the ceiling height and window height, the DSW is less adjustable and, so, was set as a fixed value of 0.2 m. Therefore, OL, EL, and TA were set as the variables. When analyzing the influence of OL on energy consumption, EL was set as 0 m, 0.2 m, 0.4 m, and TA was set as 90°. When discussing the effect of EL on energy consumption, OL was set as 0.3 m, 0.6 m, 0.9 m, and 1.2 m, and TA was set as 90°. When exploring the impact of TA on energy consumption, OL was set as 0.3 m, 0.6 m, 0.9 m, and 1.2 m, and EL was set as 0.2 m.

- Window–wall ratio (WWR)

The effect of the window–wall ratio on building energy consumption is contradictory in winter and summer. More solar radiation can be obtained in winter when increasing the window area, which benefits in improving the indoor thermal environment, but it is easy to raise the cooling energy consumption in summer. Therefore, a reasonable window–wall ratio should be required in the premise by meeting the demands of ventilation, natural lighting, and structure. The effect of window–wall ratio on building energy consumption was simulated for both south and north sides. When the south window–wall ratio was set as a variable, the north window–wall ratio was set as 0, and vice versa. Considering the influence of window thermal performance, four types were selected for the interaction analysis. The parameter settings for window–wall ratio is given in Table 8.

Table 7. Parameter settings for the external shading system.

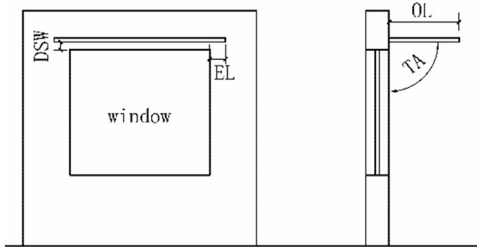
Diagram	Parameter Name	Range	Step Size
	Overhangs length of sunvisor (OL)	0–1.5 m	0.1
	Extension length of sunvisor (EL)	0–0.5 m	0.05
	Tilt angle of sunvisor(TA)	45–90°	5°

Table 8. Parameter settings for window–wall ratio.

Parameter Name	Range	Step Size	Window Type
South window–wall ratio	0.1–0.7 m	0.05	NO.1, NO.2, NO.6,
North window–wall ratio	0.1–0.7 m	0.05	NO.10 in Table 6

3. Results and Discussion

3.1. Single-Parameter and Single-Objective Analysis: Quantitative Relationships between Design Parameter and Energy Consumption

The change rule of initial investment cost with design parameters is usually clear, while the quantitative relationships between design parameters and energy consumption (heating, cooling and total) are unclear, which is mainly discussed in this section.

3.1.1. Building Form Parameters

- Building orientation

The energy consumption of the baseline model was performed from the building orientation of -90° (south by east) to 90° (south by west). It can be seen in Figure 6a that, as the orientation changes within the set range, the solar radiation increased first and then decreased, while the heating energy consumption showed an opposite trend. When the orientation was 15° south by west, the heating energy consumption reached the minimum value. Compared with the maximum value in the given orientation range, it was only reduced by $1.64 \text{ kW}\cdot\text{h}/\text{m}^2$ (about 2.5%), revealing that the variation of building orientation has little effect in the Hanzhong region. This is mainly related to the solar radiation intensity, which is a small difference in east, west, and south orientation in winter (Figure 6d). Figure 6b shows that, as the solar radiation leads to increased cooling energy consumption in summer, both of them had the same change rule with orientation. The cooling energy consumption and solar radiation decreased first and then increased, reaching the minimum value when the orientation was south, which can be reduced by $5.23 \text{ kW}\cdot\text{h}/\text{m}^2$ (about 18.2%) in terms of cooling energy consumption, indicating that the change of building orientation has a great influence on cooling energy consumption. This also rests with the total solar radiation intensity in varied directions. From the view of total energy consumption, Figure 6c displays a trend of first decreasing and then increasing, differing from Figure 6a,b in that the curve was basically symmetric. When the orientation was 5° south by west, the total energy consumption achieved the minimum value, which can be reduced by $6.33 \text{ kW}\cdot\text{h}/\text{m}^2$ (about 6.8%) compared to the maximum value. These results reveal that a reasonable building orientation has a positive effect on reducing the total energy consumption.

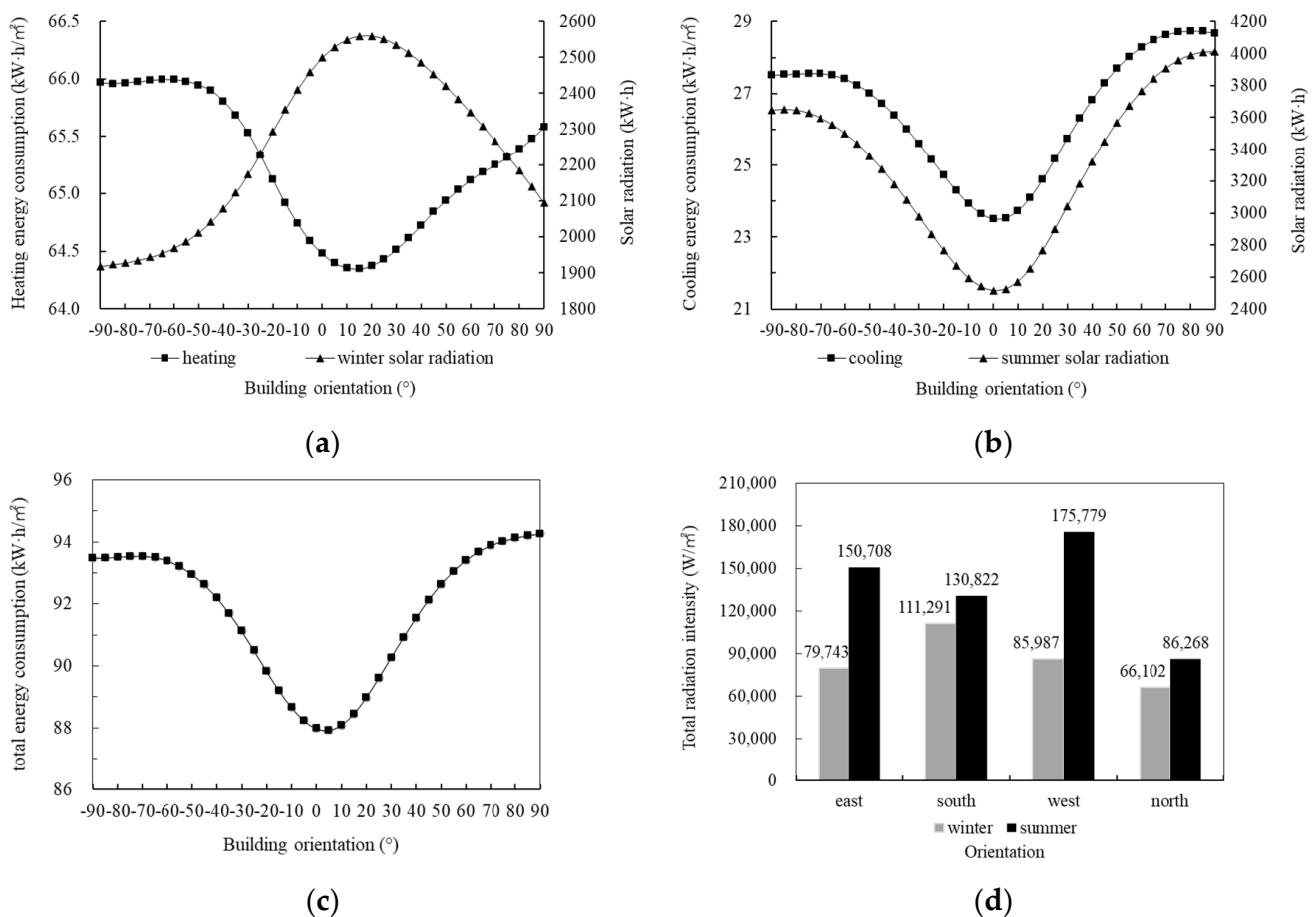


Figure 6. Relationships between building orientation and energy consumption and total radiation intensity: (a) heating energy consumption; (b) cooling energy consumption; (c) total energy consumption; (d) total radiation intensity.

- Length–width ratio (LWR)

When the value of WWR is fixed, a change in the length–width ratio will alter the south facing window area. At this time, the building energy consumption and change rule will be affected because of the difference in solar radiation. Therefore, the southward window–wall ratio was set as 0, 0.25, and 0.5 for analysis. Figure 7a shows that with an increase in the LWR, the heating energy consumption showed a trend of decreasing first and then increasing under the three conditions. However, when the energy consumption reached the minimum value, the corresponding value of WWR was different, respectively, that is 1.1, 1.3, and 1.5 under south wall–window ratios of 0, 0.25, and 0.5. In the interval of 0.7–1.1 (1.3, 1.5), the heating energy consumption had a negative correlation with LWR. In this range, the maximum fluctuations of energy consumption were 0.4 kW·h/m², 0.7 kW·h/m², and 1.0 kW·h/m², respectively. It indicates that, when the window–wall ratio was 0.5, the LWR had a larger influence on the energy consumption. With the scope of 1.1 (1.3, 1.5)–2.5, it showed an opposite trend. The maximum fluctuations of energy consumption in this interval were 2.1 kW·h/m², 1.4 kW·h/m², and 1.0 kW·h/m², respectively. As displayed in Figure 7b, with the increase of LWR, different change trends were discovered for the cooling energy consumption. When the value of WWR was 0, the energy consumption decreased with an increase in LWR and the change rate decreased gradually. When the value of WWR was equal to 0.25, the energy consumption decreased first and then increased, but the variability over the whole interval was small. At the window–wall ratio of 0.5, the energy consumption increased linearly.

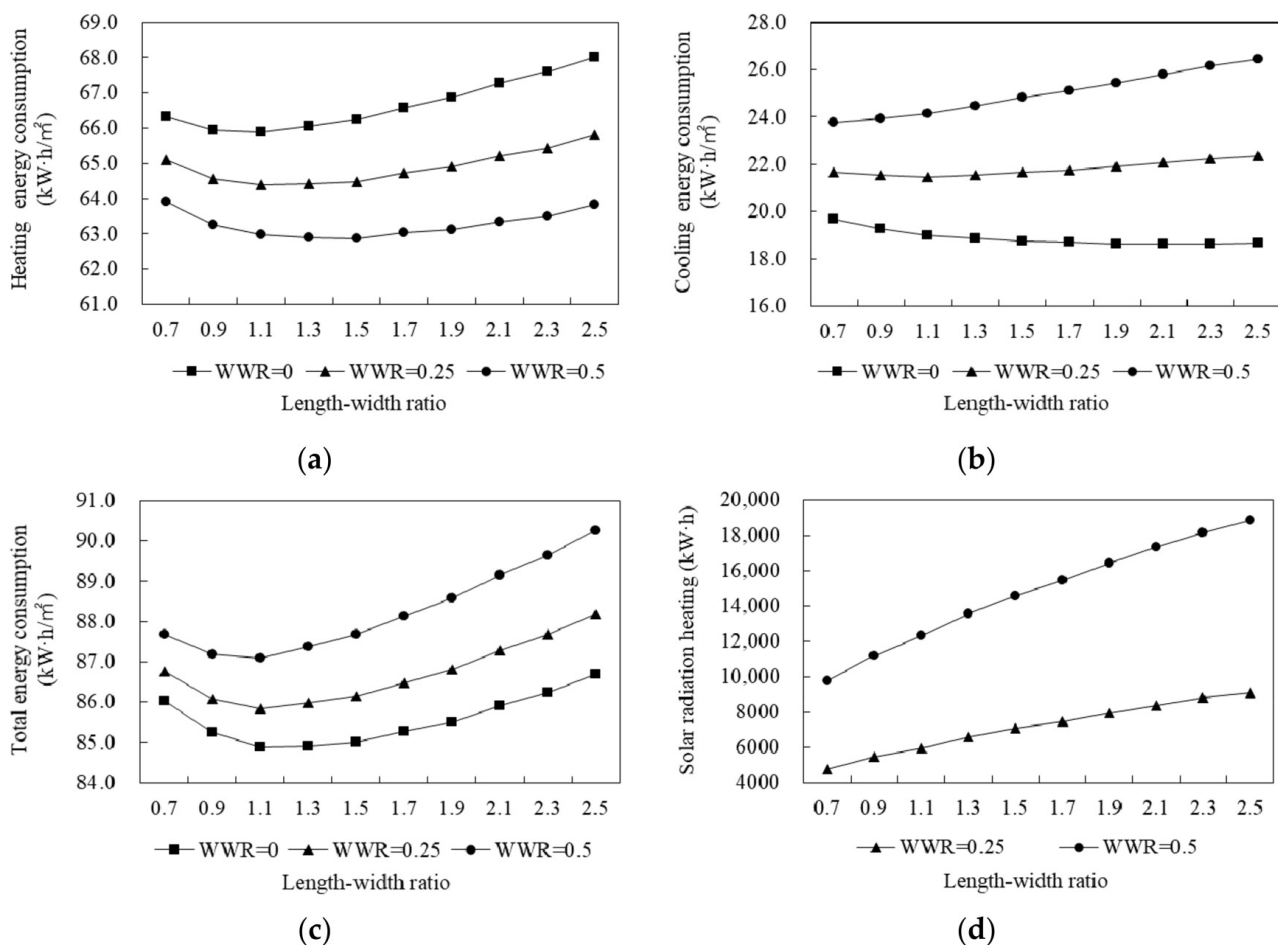


Figure 7. Relationships between length-width ratio and energy consumption and solar radiation heating: (a) heating energy consumption; (b) cooling energy consumption; (c) total energy consumption; (d) solar radiation heating.

As shown in Figure 7c, in view of the total energy consumption, it first decreased and then increased with an increase in the LWR. Interestingly, when the energy consumption reached the minimum value, the LWR was the same (1.1 m) for the three conditions. With the interval of 0.7–1.1 m, the maximum fluctuations in this interval were 1.1 kW·h/m², 0.9 kW·h/m², and 0.6 kW·h/m² under window-wall ratios of 0, 0.25, and 0.5, respectively. In particular, it had a great influence when the window-wall ratio was 0. In the range of 1.1–2.5 m, it showed the contrary tendency. The variation of LWR had a great influence under the value of 0.5 for window-wall ratio. However, the LWR is not only related to the energy consumption, but, more importantly, to meet functional requirements. A suitable length-width ratio should be determined in combination with these two aspects in design.

3.1.2. Building Envelope Parameters

• External wall and roof

As an increase in the insulation layer thickness is beneficial to reduce the heating and cooling energy consumption, this section is only analyzed from the perspective of total energy consumption, as displayed in Figure 8. With an increase in insulation layer thickness, the total energy consumption significantly decreased in the initial stage, followed by a slow decrease, and then a plateau of the curve, indicating that, when the insulation layer reaches a certain thickness, further thickening is unable to obviously reduce the energy consumption, while leading to an increase in the initial investment cost. For different materials in the same part, the better the thermal performance of the material (PUR > XPS > EPS > PER), the larger the energy consumption reduction in the initial stage. For the same material in the external wall and roof, the energy consumption was reduced more obviously for the

roof in the initial stage, that is, the curve was seemingly steeper. Taking EPS board, for instance, the reductions in energy consumption for external walls and roof respectively were $16.22 \text{ kW}\cdot\text{h}/\text{m}^2$ and $22.16 \text{ kW}\cdot\text{h}/\text{m}^2$ under the same thickness of 0.6 m . According to the external walls with different orientation, as displayed in Figure 9, it was found that as the insulation layer thickness (EPS board) increases, the effect size of each orientation on energy consumption is unequal. The north wall insulation layer had the largest impact on total energy consumption, namely having the highest sensitivity. The others were in the order of west, east, and south. This may be related to the differences of indoor solar radiation heat gain obtained from each orientation.

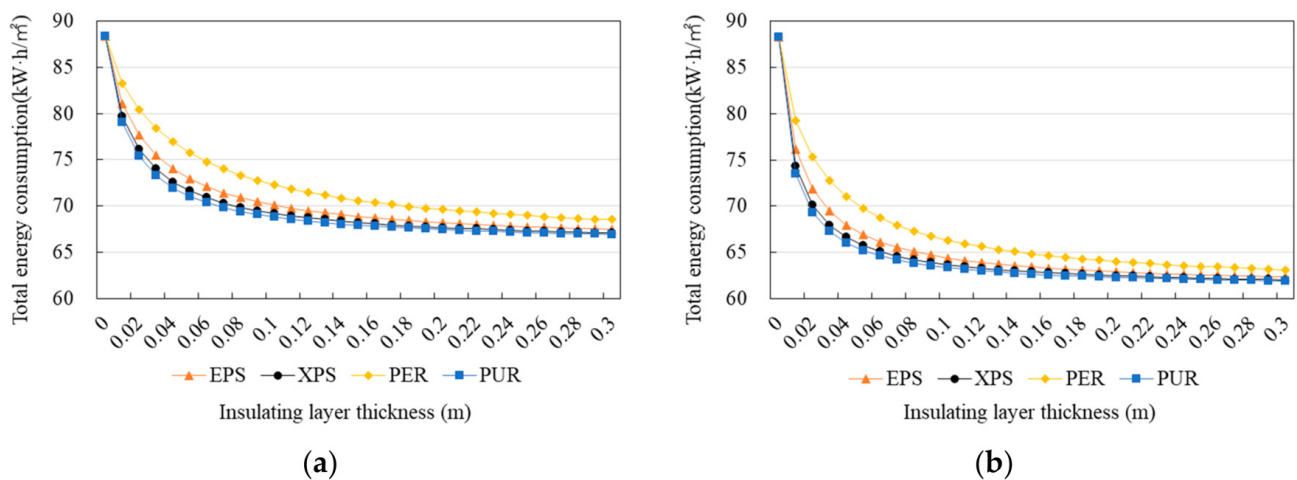


Figure 8. Relationships between insulation layer thickness and total energy consumption: (a) external wall; (b) roof.

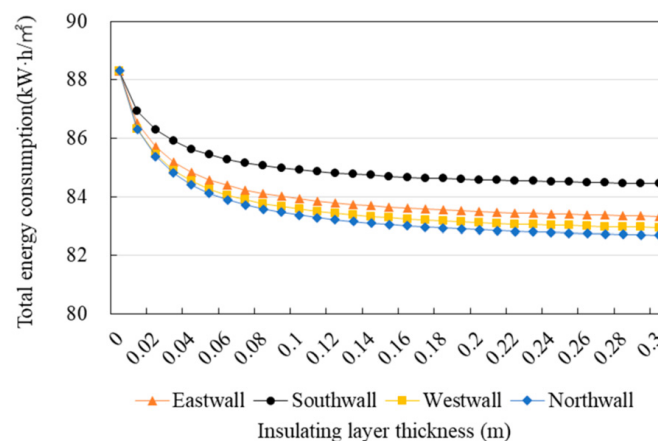


Figure 9. Relationships between insulation layer thickness and total energy consumption for four orientations.

Average indoor air temperature of the second floor without heating or cooling was simulated, in order to reveal the influence of different part's insulation. EPS board was selected in this section, and the thickness of insulation layer was set at 0.1 m . The maximum daily mean temperature occurred on July 31, and the minimum daily average temperature occurred on January 1 in Hanzhong. Hence, these two typical days were chosen as the simulation time and the results are shown in Figure 10. As regards the indoor air temperature of top floor in summer, shown in Figure 10a, the impact of external walls on the air temperature was minor. It has only a little cooling effect at time 19:00–7:00. The roof had an obvious cooling effect on air temperature, reaching the maximum at 19:00, about $3.61 \text{ }^\circ\text{C}$. In the range of 10:00–19:00, it showed an increasing trend, while presented a decreasing trend from 19:00 to 8:00. Regarding the indoor temperature in winter, as shown in Figure 10b, both external wall and roof insulation obviously improved

the indoor thermal environment. The indoor air temperature was increased by $1.06\text{ }^{\circ}\text{C}$ through external wall insulation. The effect of roof insulation on the air temperature was better than external wall. It was increased by $1.47\text{ }^{\circ}\text{C}$ on average in indoor air temperature. The enhancing effect was the most obvious at 10:00 (about $1.88\text{ }^{\circ}\text{C}$), and the least at 19:00 (about $0.92\text{ }^{\circ}\text{C}$), in contrast to the cooling effect in summer.

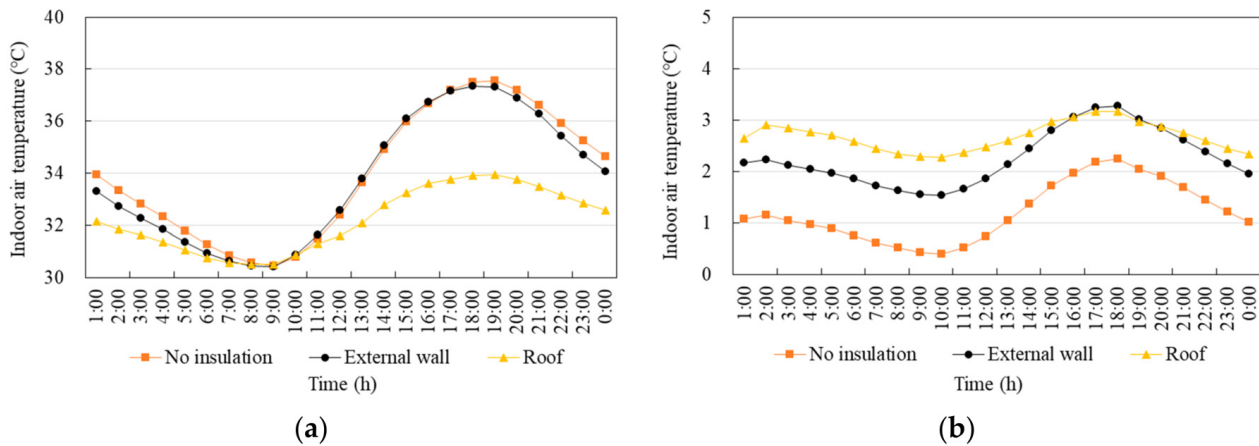


Figure 10. Air temperature variation of second floor under different insulation parts: (a) 31 July; (b) 1 January.

- External window

It can be discovered, from Figure 11, that the heating energy consumption decreased with the increase of SHGC, and vice versa for cooling in the cases of same K-values (No. 3–No. 6) and different SHGC-values. This was mainly due to the more solar radiation obtained by external windows with higher SHGC. The effect of SHGC on cooling energy consumption was higher than that for heating. For windows having the same SHGC-values (No. 6–9, No. 10–12) and different K-values, with an increase in K, the heating energy consumption increased obviously, while the cooling energy consumption decreased slightly. The change of K, thus, has a greater influence on heating energy consumption. As shown in Figure 12, as the K decreased, the total energy consumption also showed a decreasing trend, but it was not positively correlated with SHGC; mainly due to the large difference for K and small difference for SHGC.

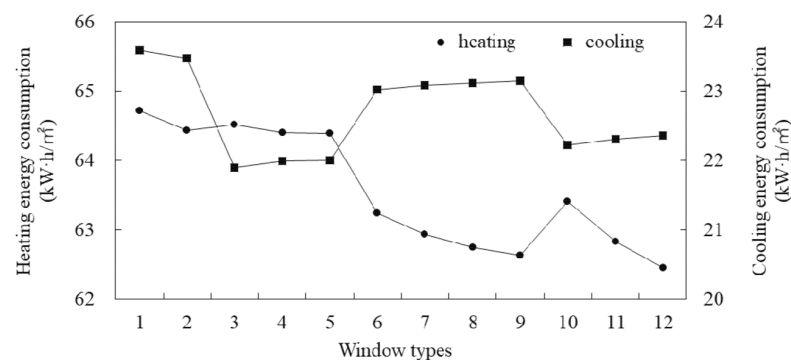


Figure 11. Relationships between window thermal performance and heating and cooling energy consumption.

SPSS was used to analyze the correlations between K, SHGC and energy consumption. It can be seen, from Table 9, that there was a significant correlation between cooling energy consumption and SHGC at 0.01 level (bilateral). Both the heating and total energy consumption were significantly correlated with K at the level of 0.01 (bilateral). This was also different from the results of a previous study [23]. Although the rural house was

located in the same climate zone, the relations between total energy consumption and K, and SHGC were different.

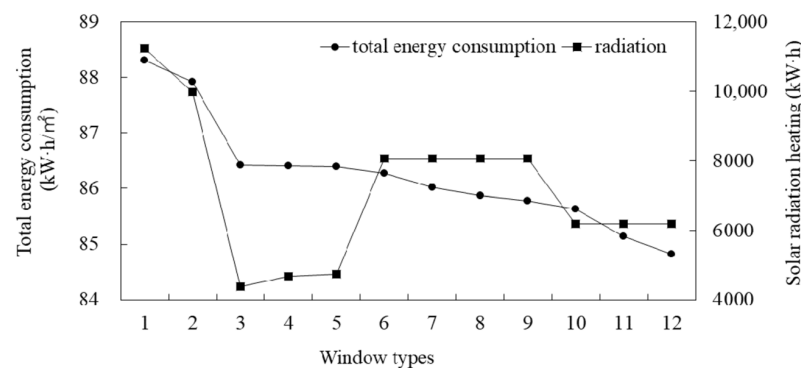


Figure 12. Relationships between window thermal performance and total energy consumption and solar radiation heating.

Table 9. Correlations between window thermal performance and energy consumption.

		K	SHGC
Heating energy consumption	Pearson correlation	0.715 **	−0.128
	Significance (bilateral)	0.009	0.692
Cooling energy consumption	Pearson correlation	0.534	0.982 **
	Significance (bilateral)	0.074	0.000
Total energy consumption	Pearson correlation	0.939 **	0.501
	Significance (bilateral)	0.000	0.097

** Significant correlation at 0.01 level (bilateral).

3.1.3. Building Interface Parameters

- External shading system

As can be seen from Figure 13a, with an increase in overhang length ($OL \geq 0.3$ m), the heating energy consumption increased linearly. As the extension length of sunvisor (EL) became longer, the change of OL had a greater impact on heating energy consumption. Figure 13b presents that, with the increase of OL, the cooling energy consumption showed a decreasing trend, with a gradually degradation of the change rate. Similarly, the longer the EL, the greater the effect of the OL. As shown in Figure 13c, the total energy consumption decreased first and then increased linearly as the OL increased. This indicates that there is an equilibrium point between heating and cooling energy consumption to minimize the total value. The corresponding value of OL was 0.6 m.

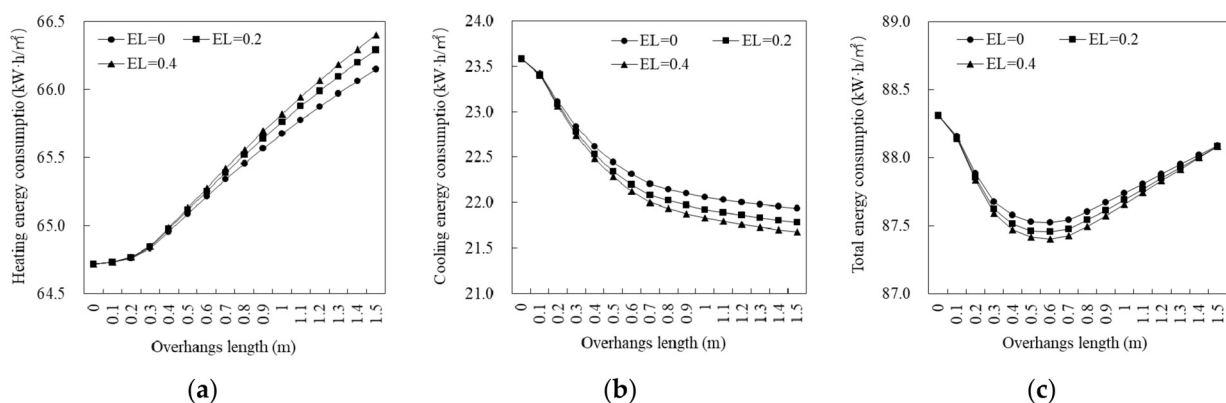


Figure 13. Relationships between overhang length and energy consumption: (a) heating; (b) cooling; (c) total.

It can be seen, from Figure 14a, that the impact of EL changing was gradually enhanced with an increase in OL. As can be seen from Figure 14b, the cooling energy consumption gradually decreased with an increase in EL. Similarly, when the OL became longer, the influence of EL also increased, but the amplitude of variation was larger than heating energy consumption. Therefore, the total value tended to decrease gradually as the EL increased, as shown in Figure 14c, but the difference is that when the OL was 0.6 m, the change of EL had the most obvious effect on the total energy consumption.

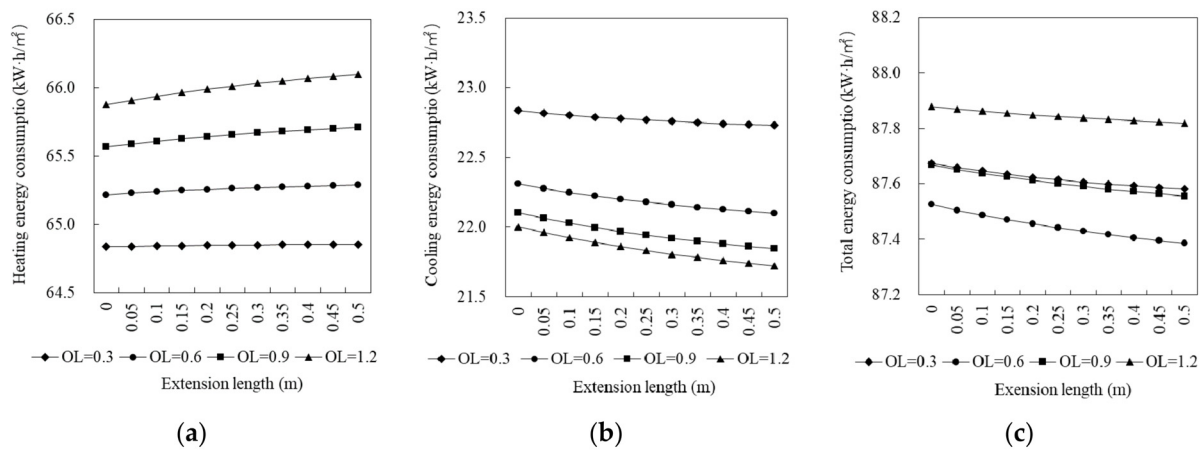


Figure 14. Relationships between extension length and energy consumption: (a) heating; (b) cooling; (c) total.

As shown in Figure 15a, the heating energy consumption showed a trend of increasing as the TA decreased. Meanwhile, the influence of decreasing TA on heating energy consumption increased gradually with an increase in OL. As shown in Figure 15b, when the OL was 0.3 m, the cooling energy consumption decreased first and then increased with a decrease in TA, but the change range is very small, and it was reduced as the TA decreased under other conditions. The increase in OL had the same effect as above, but the amplitude of variation was smaller. Therefore, the total energy consumption increased with a decrease in TA, as shown in Figure 15c. Similarly, the longer the OL in the given range, the greater the influence of reducing TA on total energy consumption. In summary, the interaction between these three parameters should be paid attention to in the design, so as to determine their optimal values.

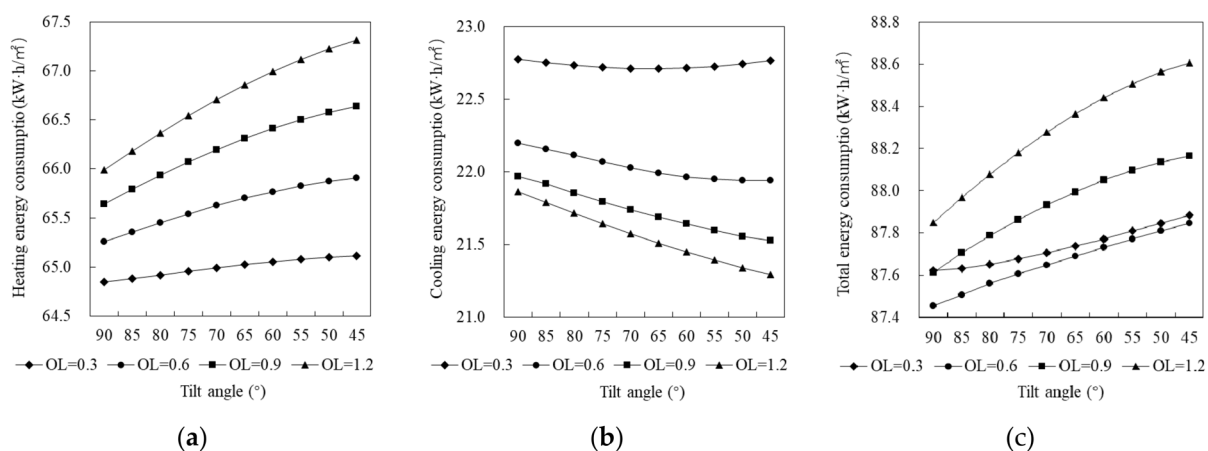


Figure 15. Relationships between tilt angle and energy consumption: (a) heating; (b) cooling; (c) total.

Through the above analysis, three parameters have different influences on the energy consumption. There is closely related between the size and cost of shading system. So, the interaction between these parameters should be considered in the design.

- Window–wall ratio

As shown in Figure 16a, the heating energy consumption decreased linearly with increasing window–wall ratio, but its rate of decline is different, due to the difference in window thermal performance. The higher the window thermal performance, the faster the rate of decline. It should be noted that, although the K-value of window type 10 is smaller than that of type 6, its SHGC-value is also smaller, making it unable to access more solar radiation (Figure 16d); thus, the heating energy consumption of type 6 is lower. As can be seen from Figure 16b, the cooling energy consumption increased with increasing window–wall ratio, and its growth rate exhibited a downward trend with the improvement of window thermal performance, as opposed to heating energy. Figure 16c shows that, when the external window was type 1, type 2, and type 6, the total energy consumption presented a trend of growing as the window–wall ratio increased. The influence of window–wall ratio on the total value decreased with the improvement of window thermal performance. However, when the external window was type 10, the total energy consumption decreased slightly with an increase in window–wall ratio, however the maximum reduction was only $0.2 \text{ kW}\cdot\text{h}/\text{m}^2$.

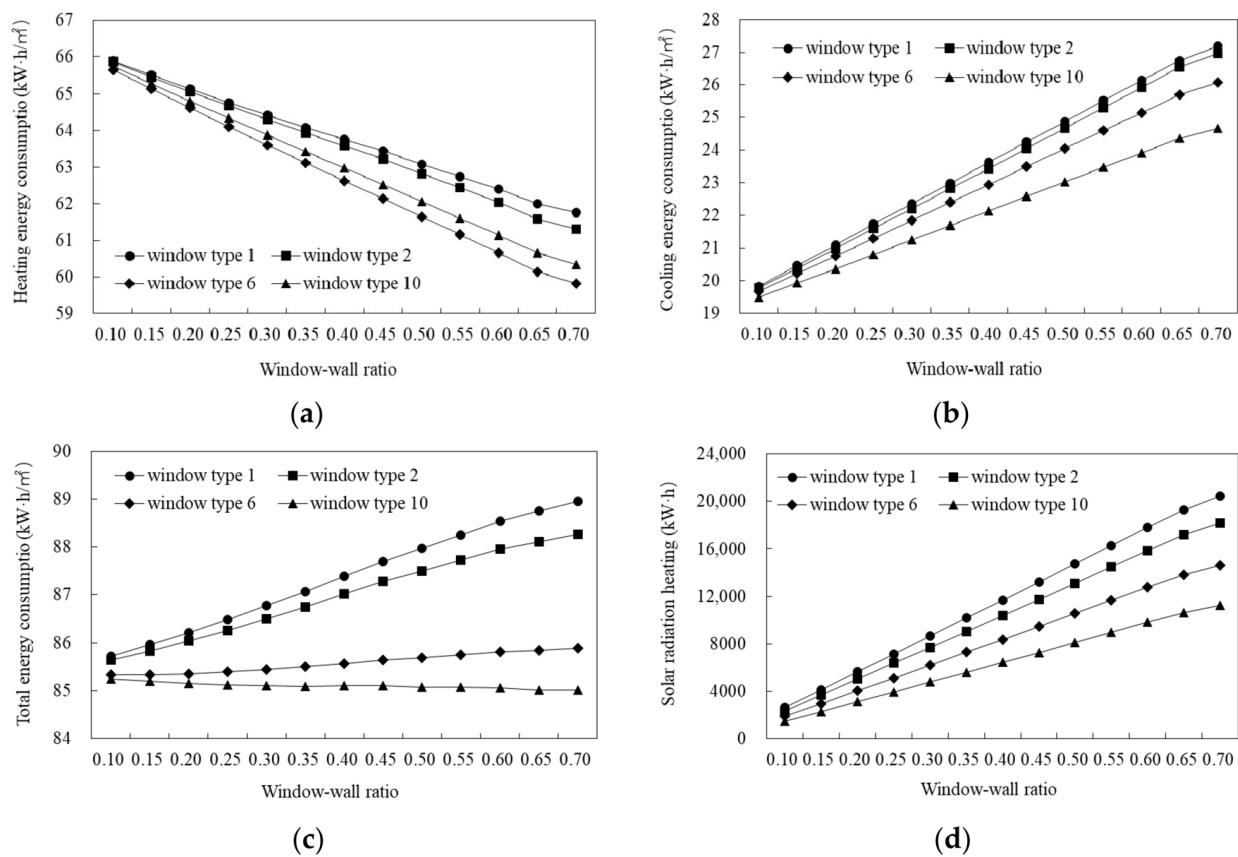


Figure 16. Relationships between south window–wall ratio and energy consumption and solar radiation heating: (a) heating energy consumption; (b) cooling energy consumption; (c) total energy consumption; (d) solar radiation heating.

As can be seen from Figure 17a, when the external window was type 1, the heating energy consumption increased first and then decreased as the window–wall ratio increases; however, the maximum variation was only $0.41 \text{ kW}\cdot\text{h}/\text{m}^2$. When the external window was type 2, type 6, and type 10, the heating energy consumption reduced with an increase in the window–wall ratio. When the value of WWR increased from 0.1 to 0.7, the reductions of heating energy consumption were $0.52 \text{ kW}\cdot\text{h}/\text{m}^2$, $2.09 \text{ kW}\cdot\text{h}/\text{m}^2$, and $2.44 \text{ kW}\cdot\text{h}/\text{m}^2$, respectively, revealing that the influence of window–wall ratio increases with the raise of window thermal performance. As shown in Figure 17b, with an increase in the window–

wall ratio, the cooling energy consumption exhibited a linearly upward trend, but with varying growth rate: the higher the thermal performance of the window, the slower the growth rate. It can be observed, from Figure 17c, that the change rule of total energy consumption was similar to that of the cooling energy consumption, just with a different growth rate.

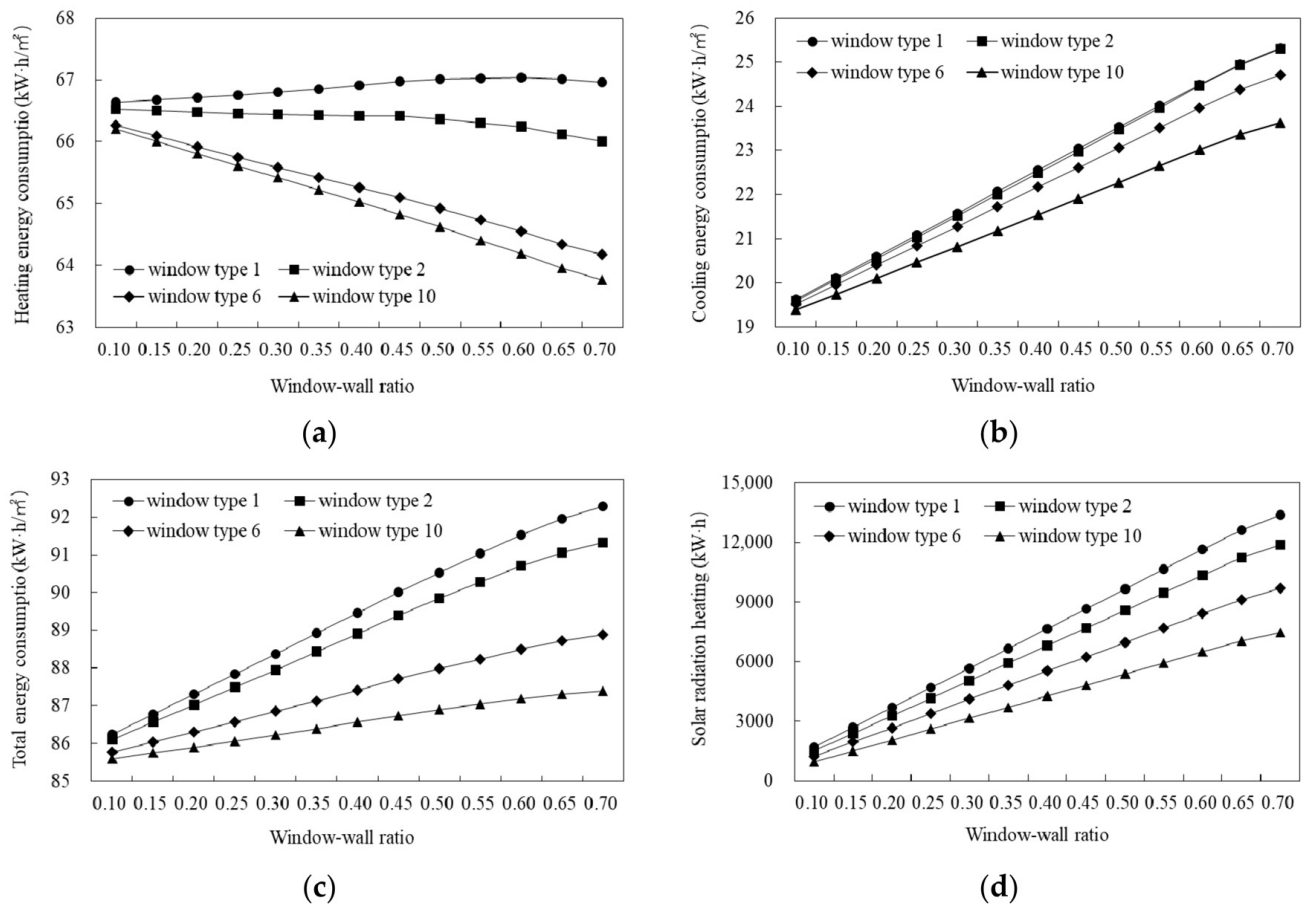


Figure 17. Relationships between north window–wall ratio and energy consumption and solar radiation heating: (a) heating energy consumption; (b) cooling energy consumption; (c) total energy consumption; (d) solar radiation heating.

Based on the analysis in previous sections, it can be concluded that the north window–wall ratio is more sensitive to total energy consumption. Taking window type 1 for example, for every 0.1 increase in the south window–wall ratio, the total energy consumption increased by 0.27 kW·h/m²; meanwhile, for every 0.1 increase in the north window–wall ratio, it increased by 0.5 kW·h/m².

3.2. Multi-Parameters and Multi-Objective Optimization: Parameters Combination Based on Energy Consumption and Initial Investment Cost

According to the single-parameter and single-objective analysis, it was found that the influence of each design parameter on energy consumption was different. There were also interactions between the design parameters; that is, the influence of one factor on the energy consumption may vary with the parameters of other factors, such that the univariate analysis may be one-sided. In addition, reducing energy consumption also brings about the problem of increased investment cost. Therefore, all kinds of design parameters needs to be considered simultaneously, in terms of both energy saving and initial investment cost.

3.2.1. Objective Functions

Multi-objective optimization is a method to scientifically and rationally select multiple contradictory objectives and then make a decision. According to the multi-objective problem, one solution may perform optimally on a particular target, but may perform poorly in other objectives, such that it is difficult to use a unique optimal solution to represent it. The essential difference between multi-objective and single-objective optimization is that there is no unique solution to make all objectives optimal; instead, we search one or more satisfactory solutions acting as a compromise between the objectives. These solutions are called Pareto optimal solutions (or Pareto non-dominant solutions). In this study, two objectives are considered, namely, total energy consumption and initial investment cost. The goal was to identify the optimal values of multi-parameters under the interactions between the above two objectives.

- Total energy consumption

In accordance with the analysis results of Section 3.1, some design parameters had opposite effects on heating and cooling energy consumption. For example, increasing the south window–wall ratio benefits in reducing the heating energy consumption, but will increase the cooling energy consumption. Therefore, the heating and cooling energy consumptions were superimposed, and the total energy consumption was set as the optimization objective, so that the parameters of the design variables can take into account both the demands. The total energy consumption was output by the EnergyPlus software.

- Initial investment cost

There is a large gap between the rural and urban economic levels, which should also be considered while meeting the energy saving requirements for rural buildings. Economy is a key factor affecting the energy saving design for rural houses. Therefore, the initial investment cost was set as another optimization objective. As the load-bearing structure and the cost of labor and transportation of different design schemes are basically the same, the initial investment cost does not need to calculate the absolute value, but only the incremental cost caused by the energy-saving design of each part (dIC). This value can be calculated by Formula (2):

$$dIC = \sum_{i=1}^i dIC_i = \sum_{i=1}^i S_i \times dP_i \quad (2)$$

where dIC_i is the incremental cost of each part, S_i is the area of adopting energy-saving measures of each part, and dP_i represents the material price difference of each part.

In conclusion, the objective function of multi-objective optimization can be expressed as Formula (3). Its aim is to jointly make the two function values as small as possible.

$$\text{Min } \{f_1\bar{x}, f_2\bar{x}\}, \bar{x} = [x_1, x_2, \dots, x_N] \quad (3)$$

where f_1 is the total energy consumption (kW·h/m²), f_2 is the initial investment cost (yuan), and \bar{x} denotes the parameters combination of design variables.

3.2.2. Design Variables

Seventeen variables are considered in this study, including building orientation, height and width of south and north windows (six variables), insulating layer thickness of wall and roof (five variables), type of insulation material, window type (with different K and SHGC values), and external shading parameters (three variables). The value interval of each variable was set in line with the above analysis in Section 3.1. Table 10 provides the list of variables, as well as their symbol, range of variation, step, and initial value. In order to avoid the impact on indoor daylighting, the minimum window area values were imposed to meet the requirements of window–floor ratio for bedrooms, living rooms, and kitchen given in the <Design code for residential buildings (GB 50096)>. In addition, according to the analysis results of Section 3.1.1, the length–width ratio was set in advance, and not

selected as an optimization variable. According to the requirements of plane layout and building area, the plane size was set as 12.3 m × 8.1 m, as shown in Figure 3, and the corresponding length–width ratio was 1.5. Although it was not the optimal length–width ratio of 1.1, the energy consumption was also in the lower range. The investment costs for different materials are shown in Table 11. The material prices were estimated after marking market inquiries and a network survey.

Table 10. Parameter settings for the design variables.

Parameter Name	Symbol	Range	Step Size	Initial Value	Variable Type
Building orientation (°)	o	[−30, 30]	5	0	continuous
Width of south window (m)	ws	[1.8, 2.7]	0.1	2.4	continuous
Height of first floor south window (m)	hsf	[1.5, 2.2]	0.1	1.8	continuous
Height of second floor south window (m)	hss	[1.5, 1.8]	0.1	1.8	continuous
Width of north window (m)	wn	[1.5, 2.1]	0.1	1.5	continuous
Height of first floor north window (m)	hnf	[1.5, 2.2]	0.1	1.5	continuous
Height of second floor north window (m)	hns	[1.5, 1.8]	0.1	1.5	continuous
Insulation materials	im	2	—	NO.1	discrete
Insulation thickness of south wall (m)	ts	[0, 0.2]	0.01	0	continuous
Insulation thickness of north wall (m)	tn	[0, 0.2]	0.01	0	continuous
Insulation thickness of east wall (m)	tw	[0, 0.2]	0.01	0	continuous
Insulation thickness of west wall (m)	te	[0, 0.2]	0.01	0	continuous
Insulation thickness of roof (m)	tr	[0, 0.2]	0.01	0	continuous
Window type (K, SHGC)	win	3	—	NO.1	discrete
Overhangs length of sunvisor (m)	ol	[0, 1.5]	0.1	0.9	continuous
Extension length of sunvisor (m)	el	[0, 0.5]	0.1	0.2	continuous
Tilt angle of sunvisor (°)	ta	[45, 90]	5	90	continuous

Note: The number 2 in the range column for insulation materials represents two types of materials, namely EPS board and XPS board. The number 3 in the range column for window type represents three types of materials, namely type 2, type 6, type 10 (see Table 6). The external windows of the staircase and toilet were set as fixed values. The south window–wall ratio is expressed as SWWR and the north window–wall ratio is expressed as NWWR.

Table 11. The investment costs of different design options.

Parts	No.	Materials	Performance Parameters	Price
External wall, roof	1	Expanded polystyrene board (EPS)	$\lambda = 0.040 \text{ W/m}\cdot\text{K}$	360 ¥/m ³
	2	Extruded polystyrene board (XPS)	$\lambda = 0.030 \text{ W/m}\cdot\text{K}$	480 ¥/m ³
Window	1	Single Low-e clear 6 mm	$K = 3.8 \text{ W/m}^2\cdot\text{K}$, SHGC = 0.72	200 ¥/m ²
	2	6 mm clear + 6A + 6 mm clear	$K = 3.1 \text{ W/m}^2\cdot\text{K}$, SHGC = 0.70	260 ¥/m ²
	3	6 mm clear + 6A + 6 mm Low-e	$K = 2.4 \text{ W/m}^2\cdot\text{K}$, SHGC = 0.57	350 ¥/m ²
External shading	1	Concrete slab	—	100 ¥/m ²

Note: Among the four thermal insulation materials, PER has a poorer thermal insulation performance, while PUR has a stronger thermal insulation performance but a higher price, so the XPS and EPS were selected as the optimization variables. The window frame was made of plastic steel and the thickness of glass was 6 mm. The window price for the baseline building is 100 ¥/m².

3.2.3. Analysis of Pareto Solutions

- Correlation and value distribution of multi-objectives

As shown in Figure 18 and Figure 19, the Pareto solutions, which are the parameter combinations based on optimization of total energy consumption and initial investment cost (including 29 groups), were obtained using the NSGA-II algorithm with 2016 iterations. As displayed in Figure 19, the total energy consumption showed a decreasing trend as the initial investment cost increases, indicating a mutual exclusion between the two objectives. This was mainly due to the 17 design variables, except for building orientation, the others are directly related to the investment cost, such as the addition of insulation materials to the external wall and roof, adoption of high-performance windows, and installation of sunvisor, etc. These measures can improve the efficiency of energy conservation, but will inevitably lead to an increase in the investment cost.

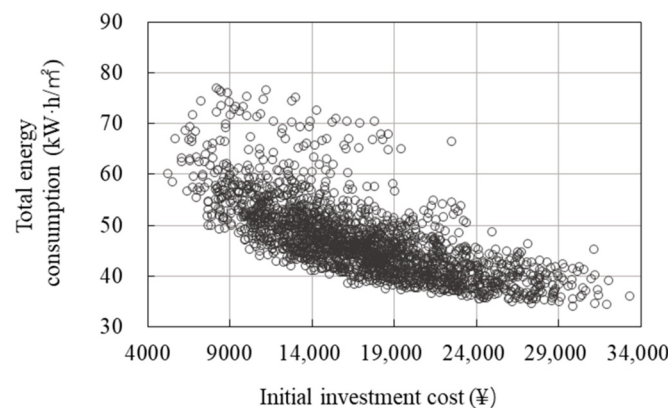


Figure 18. Iterative operation process of bi-objective optimization.

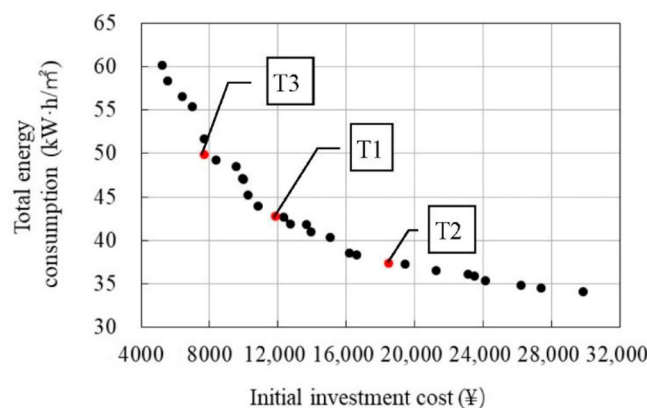


Figure 19. Pareto front of bi-objective optimization.

As can be seen in Figure 19, from the value distribution of two objectives, the Pareto solutions of total energy consumption ranged from 34.0 kW·h/m² to 60.1 kW·h/m². The optimum solution was 34.0 kW·h/m², while the worst one was 60.1 kW·h/m², and there was a difference value of 26.1 kW·h/m² to the maximum when choosing the solutions. Compared with the baseline model, the energy saving rate varied from 61.5% to 31.9%. The initial investment cost of Pareto solutions was distributed at ¥ 5271.8–¥ 29,902.2, where the difference between the maximum and minimum values was ¥ 24,630.4. In terms of the relationship between the two objectives, under the minimum initial investment cost of ¥ 5271.8, the corresponding energy saving rate was 31.9%, and the maximum initial investment cost of ¥ 29,902.2 corresponded to an energy saving rate of 61.5%. It also can be discovered, from Figure 19, that when the initial investment cost was less than ¥ 12,000.0, with an increase in the initial investment cost, the total energy consumption decreased significantly, and the energy saving rate increased from 31.9% to 51.5%, with an increment of about 19.6%. When the initial investment cost was more than ¥ 12,000.0, with continued increase in the initial investment cost, the energy saving rate increased from 51.5% to 61.5%, an increment of only about 10%.

- Value distribution of design variables

On the basis of the Pareto solutions obtained from multi-objective optimization, the value distribution of each design variable was counted, as shown in Figure 20. For the building orientation, within the given threshold range, it was mainly distributed in the range of -20° – 10° —that is, from 20° south by west to 10° south by east—among which 89.7% of results were concentrated between 0° and 10° . As the building orientation is unlimited by cost, this was consistent with the single-parameter analysis.

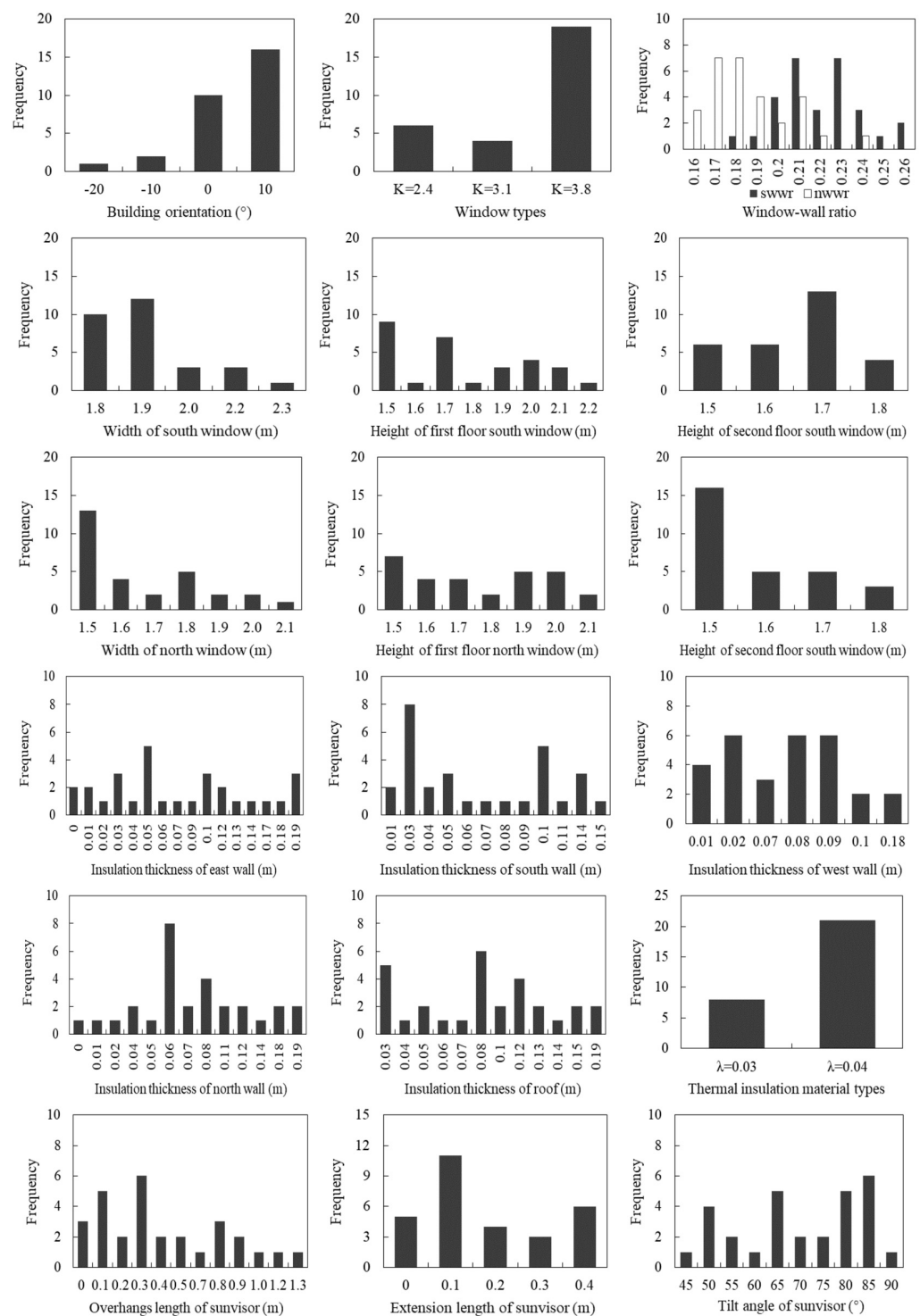


Figure 20. Value distributions for all design parameters.

Regarding the external window type, under the constraint of investment cost, the single Low-e clear 6 mm (No. 1 in Table 11) was adopted in most solutions, accounting for 65.5%. In terms of the window size, the width of south window ranged from 1.8 m to 2.3 m, not reaching the upper limit value of 2.7 m. It was mainly concentrated in 1.8 m and 1.9 m, accounting for 75.9% of solutions. The height of south window was distributed within the full threshold, and there were three extreme points of 1.5 m, 1.7 m, and 2.0 m for the height distribution of the first floor window, accounting for a larger proportion of 68.9%. For the second floor window, the height of 1.7 m was the most common, accounting for 44.8%. The south window–wall ratio was distributed in the range of 0.18–0.26, among which 82.8%

varied from 0.2 to 0.24. Under the comprehensive action of design variables, the area of south window should be neither too large nor too small. For the north window, the height and width were both distributed within the full threshold. There were two extreme points of 1.5 m and 1.8 m for the width of window, accounting for 62.0%. The height distribution of the first floor window was relatively uniform, while that of the second floor window tended to the lower limit, with a percentage of 55.2% for the 1.5 m height in most. The north window–wall ratio was distributed in the range of 0.16–0.24, among which 72.4% varied from 0.16 to 0.19. The area of north window was relatively small.

Considering the external wall and roof, both types of insulation materials were used. Similarly, limited by the initial investment cost, the EPS board (with lower price) accounted for 72.4%. Under the restriction of dual objectives, the insulation layer thickness of Pareto solutions did not reach the upper limit of the threshold. This was mainly due to the fact that, although increasing the thickness is beneficial to reduce energy consumption, such reduction gradually decreases, while the initial investment cost still increases linearly. However, the value distribution of insulation layer thickness in different parts was not the same. In terms of the value interval, the ranges of insulation thickness for south, west, east, and north walls were 0.01–0.15 m, 0.01–0.18 m, 0–0.19 m, and 0–0.19 m respectively. This was mainly due to the relatively low sensitivity of south wall insulation thickness to the influence of energy consumption, such that it should not be too thick under the restriction of investment cost. The range of insulation thickness for roof was 0.03–0.19 m, where its minimum value was higher than the external wall, mainly as the energy-saving effect of roof insulation was more obvious at the same insulation thickness. From the view of value distribution, the two variables of east and south wall insulation thickness, with low sensitivity, tended to the upper and lower limits of the threshold. 0.05 m and 0.1 m were taken as the boundaries, and those with $t_e \leq 0.05$ m accounted for 48.3% and $t_e \geq 0.1$ m accounted for 41.4%, while the number with $t_s \leq 0.05$ m accounted for 51.7% and $t_s \geq 0.1$ m accounted for 34.5%. With regard to the two variables with high sensitivity, the values of west and north wall insulation thickness tended to develop in one-way dimension, that is, 86.2% of the $t_w < 0.1$ m and 79.3% of the $t_n > 0.05$ m. The insulation thickness of roof also developed in two dimensions, with the percentages of $t_r = 0.03$ m and $t_r \geq 0.8$ m being 17.2% and 65.5%, respectively.

About the external shading system, the overhang length (OL) and extension length (EL) unreached the upper limits of their respective threshold. The range of OL was 0–1.3 m, which tended to the lower the limit. The percentage of $OL \leq 0.9$ was 89.7% (69.0% of the $OL \leq 0.5$). The EL was distributed from 0 to 0.4 m, and the value tended to two dimensions of upper and lower limits. The values near the lower limit took up a large proportion, with a percentage of $el \leq 0.1$ at 55.2%. The title angle (TA) of sunvisor was distributed in the full threshold, and there were several extreme points, such as the number of $ta = 50^\circ$, $ta = 65^\circ$, and $ta = 80^\circ$ and 85° accounted for 13.8%, 17.2%, and 37.9%, respectively.

- First parameter combinations of different patterns

Although Pareto solutions put forward a series of schemes to provide designers with more possibilities, a final decision is needed to determine a suitable solution. In the actual design process, design parameters are usually determined considering the wishes of the decision-maker, in order to form different design schemes. For example, rural residents are more inclined to consider the initial investment cost, while designers pay more attention to the energy saving rate. In this section, the weighted sum method (see Section 2.4) is used to determine the optimum solution for multi-objective decision problem from Pareto solutions, that is, by assigning weight coefficients to the dual objectives, the parameter combinations under different goal orientations can be obtained.

Figure 21 presents the optimum values of two objectives with different weights. Note that “Weight” represents the weight of total energy consumption. For example, “Weight = 0.1” indicates that the weights for the total energy consumption and the initial investment cost are 0.1 and 0.9, respectively, namely $w_1(\text{EC}): w_2(\text{IC}) = 1:9$. As shown in Figure 21, with

an increase in the weight value, the total energy consumption decreases and the initial investment cost increases corresponding to the optimum scheme.

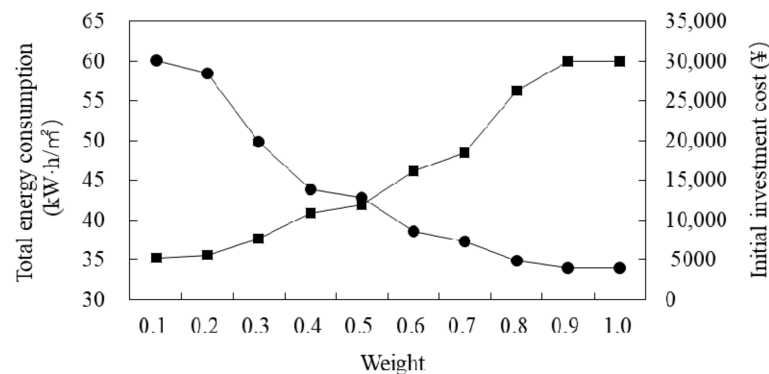


Figure 21. Impact of weight on the optimum values of total energy consumption and initial investment cost.

According to Figure 21, three typical schemes with different weight coefficients were chosen for a more detailed analysis, including: T1—both objectives have the same weight, namely $w_1(\text{EC}):w_2(\text{IC}) = 1:1$; T2—the weight of total energy consumption is higher than the initial investment cost, namely $w_1:w_2 = 2:1$; and T3—the weight of initial investment cost is higher than the total building energy consumption, namely $w_1:w_2 = 1:2$. Table 12 presents the optimum design parameters and corresponding value of two objective functions. The corresponding points are shown in Figure 19.

Table 12. Optimum design parameters and corresponding values of objective functions.

Variables	Unit	T1	T2	T3
Initial investment cost	¥	11,860.6	18,501.6	7715.3
Total energy consumption	kW·h/m ²	42.8	37.3	49.9
o	°	0	0	0
tr	m	0.13	0.12	0.05
ts	m	0.03	0.10	0.03
te	m	0.03	0.09	0.05
tn	m	0.06	0.19	0.05
tw	m	0.08	0.09	0.01
im		0.04	0.04	0.04
ol	m	0.8	0.3	0.2
el	m	0.3	0.0	0.2
ta	°	90	80	65
win		3.8	3.1	3.8
ws	m	1.9	1.9	1.8
hsf	m	1.5	1.7	1.7
hss	m	1.7	1.5	1.7
Asw	m ²	15.39	15.01	15.30
wn	m	1.5	1.5	1.8
hnf	m	2.0	1.5	1.9
hns	m	1.7	1.7	1.5
Anw	m ²	11.10	9.60	12.24

Note: Asw represents the south window area, Anw represents the north window area.

As shown in Table 12, from the view of comprehensive performance, the total energy consumption and initial investment cost are equally important in the T1 scheme. The energy saving rate is 51.5% and the initial investment cost is ¥11,860.6, which is located in the middle area of Pareto solutions. From the designer's perspective, the T2 scheme focuses on reducing the total energy consumption. Compared with T1, the energy saving rate is increased to 57.8%, and the initial investment cost is raised to ¥18,501.6. The T3

scheme, which takes the user's perspective, focuses on decreasing the initial investment cost, which is reduced to ¥7715.3 compared with T1 scheme, but the energy saving rate is decreased to 43.5%. Therefore, according to the wills of different decision-makers, the optimal design scheme selected from the Pareto solutions is different, such that there are some differences in the value of the corresponding design variables. For instance, the insulation materials used in three schemes were EPS boards, while the insulation layer thickness of external wall and roof varied greatly, thus forming a double guide control for the total energy consumption and initial investment cost. In terms of window type, the T2 scheme, which focuses on reducing the energy demand, adopts external windows with better performance. However, the area of south window was very similar under the three schemes, while the area of north window obviously differed. In the actual design process, the optimal scheme can be determined by considering the specific situation. In general, T1 is the optimal solution. For a household with relatively poor economic conditions, the T3 scheme, with low initial investment cost provides a better choice. In the contrary situation, the T2 scheme with higher energy saving rate can be selected.

In addition, the special condition where the weighted values (F) of several schemes are very similar may occur, such as when $w1:w2 = 1:1$. The F values of two more schemes were close to T1, expressed as T1-1 (is the T1, $F = 0.3023$), T1-2 ($F = 0.3027$), and T1-3 ($F = 0.3031$). It is noteworthy that, when the value of objective function is very close, the corresponding values of some design variables were still different, indicating that the complementary values of these design variables can achieve the same effect. The energy saving rates of T1-1, T1-2, and T1-3 were 51.5%, 50.1%, and 52.5%, with initial investment costs of ¥ 11,860.6, ¥ 10,841.2, and ¥ 12,755.7, respectively. With regard to the values of design variables, the insulation material and window type used in three schemes were the same, and other design variables were mutually restrictive. A parameter change of one variable will cause a change in others. The thickness of the insulation layer, parameters of the shading system, size and area of external window of these three schemes are shown in Figure 22.

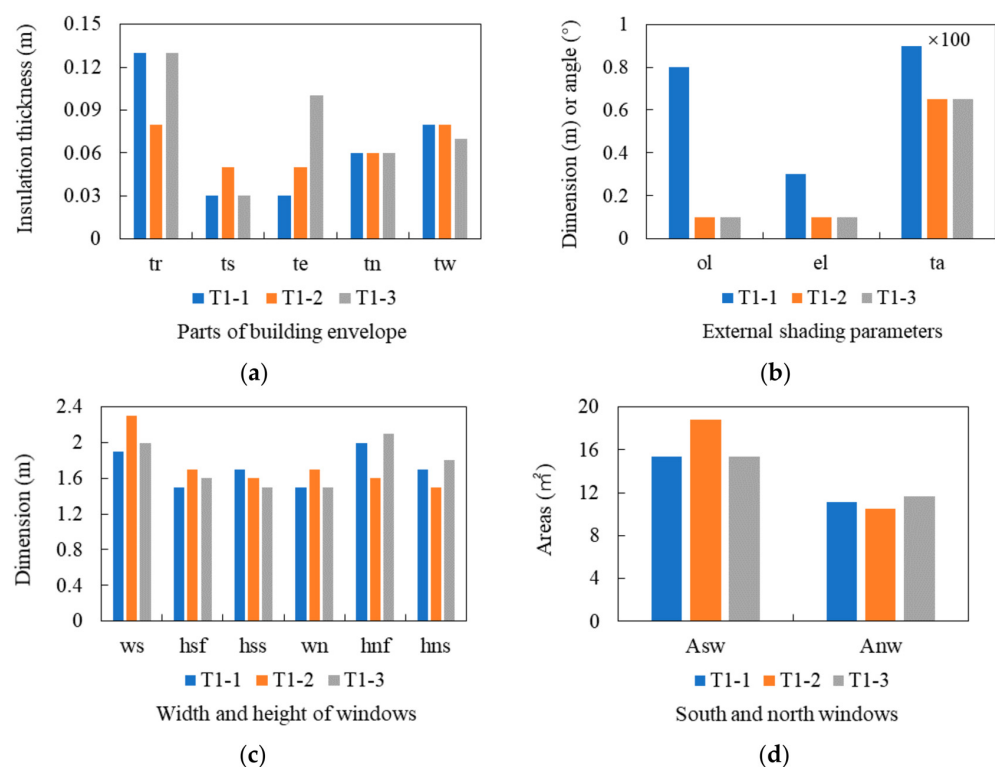


Figure 22. The design parameters under the three schemes: (a) thickness of insulation layer; (b) external shading parameters; (c) width and height of windows; (d) size of south and north windows.

Comparing T1-1 to T1-3 schemes, the building orientation of two schemes was consistent, with the parameter of 0° . In terms of insulation thickness, t_r , t_s , and t_n were the same. The t_e of T1-1 scheme was significantly less than that of T1-3, while t_w was slightly greater. Thus, the heat transfer loss of external wall will be higher than that of T1-3, so it is necessary to alter the parameters of the external window and shading system to comply with the change of total energy consumption. For the window scale, the area of south window was basically the same, while the north window area of T1-1 was less than T1-3. About the shading system, the OL, EL, and TA under the T1-1 scheme were all greater than T1-3. According to the relationship between single parameters and energy demand analyzed in Section 3.1.3, the parameters of north window and shading system are conducive to reduce the total energy consumption in the T1-1 scheme, so that T1-1 and T1-3 can achieve the same effect under the comprehensive action of design parameters. Similarly, T1-1 and T1-2 schemes also had the same orientation. For the insulation thickness, t_n and t_w were the same. The t_s and t_e of T1-1 scheme were less than that of T1-2, while t_r was thicker. Regarding the shading system, the OL, EL, and TA under the T1-1 scheme were still greater than T1-2. In terms of window scale, the south window area of T1-1 was significantly smaller than that of T1-2, while the north window area was slightly larger. With respect to the T1-2 and T1-3 schemes, the building orientations of two schemes were 10° and 0° , respectively. The shading system parameters were consistent. Other parameters, such as t_n was the same; t_r and t_e of T1-2 scheme were significantly lower than that of T1-3, while t_s and t_w were slightly greater. The south window area of T1-2 scheme was obviously larger than T1-3, while the north window was slightly smaller.

Considering the above conditions, it is equivalent to provide a variety of possibilities for the selection of a design scheme. At this time, the optimal scheme can be determined, according to the design parameters that have differences between the different schemes. These parameters can be divided into two categories: (1) Functional parameters, such as insulating layer thickness and window type (K, SHGC), which only affect the energy consumption and investment cost, but do not affect the building appearance and indoor layout; and (2) synthetic parameters, such as the parameters of external window scale and shading system, which not only affect the energy consumption and cost, but also have an impact on the building style or layout. The decision of a suitable scheme mainly depends on preference regarding the second category of parameters. Taking the above three schemes as an example, as shown in Figure 22b, if a larger overhang length of the sunvisor is preferred, T1-1 scheme is the best choice. The south window scale also can be used as a screening condition, as shown in Figure 22c,d, e.g., T1-2 may be the optimal scheme on the premise of preferring larger south window area. It should be noted that the weighted values mentioned here are only very close, not completely equal. If there is no special requirement, the scheme with the minimum weighted value should be preferred.

4. Conclusions

In this paper, based on the climate conditions of Hanzhong area (hot summer and cold winter), we carried out the single-parameter and single-objective analyses, followed by the multi-parameter and multi-objective optimization of rural houses from the perspective of passive building energy-saving design. According to the research findings, the following conclusions can be drawn:

Based on the quantitative analysis results between single-parameter and heating, cooling and total energy consumption, the effect rule of each parameter on can be clarified as follows: ① When the orientation rotates from -90° to 90° , the total energy consumption decreases first and then increases. When the orientation is 5° south by west, it reaches the lowest energy consumption, with corresponding energy saving rate of 6.8%. ② With an increase in LWR, the total energy consumption decreases first and then increases. When the energy consumption reaches the lowest value, the corresponding length–width ratio is 1.1. ③ For the external wall and roof, the total energy consumption is reduced more obviously for the roof insulation than that of the external wall in the initial stage. The

influence of external wall insulation thickness on energy consumption also varies with the orientation, where the north wall has the greatest sensitivity. Adding insulation to the roof has a significant cooling effect on the indoor temperature of second floor in summer. For the winter, the indoor temperature can be obviously improved by both wall and roof insulation, where roof insulation has a better effect. ④ Regarding the external windows, the total energy consumption is significantly correlated with the K-value at the level of 0.01; whereas there is no significant correlation with the SHGC-value. ⑤ With the increase of OL, the total energy consumption first decreases gradually, then increases linearly. As a raise in EL, it tends to gradually decrease, but the difference is that, when the OL is 0.6 m, changing the EL has the most obvious effect. As the TA decreases, it shows an increasing trend. ⑥ With an increase in south WWR, the change rule of total energy consumption presents different trends with changing window thermal performance. With the increase in north WWR, the total energy consumption exhibits a linearly increasing trend, the higher the window thermal performance, the slower the growth rate. Comparing to the south WWR, the north WWR has greater sensitive to the total energy consumption.

It is necessary to consider the synergistic effect of multiple parameters in terms of the total energy consumption and initial investment cost. Through 2016 iteration operations, Pareto solutions were obtained. Results demonstrated that, with a decrease in total energy consumption, the initial investment cost increases gradually, and there exists a mutual exclusion between the two objectives. At the minimum initial investment cost of ¥ 5271.8, the corresponding energy saving rate is 31.9%, while at the maximum initial investment cost of ¥ 29,902.2, the energy saving rate reaches 61.5%, with a variation range of 29.6%. Through an impact analysis of weight on the optimum values of total energy consumption and initial investment cost, three typical design schemes were screened from the Pareto solutions to meet the preferences of different decision-makers in detailed analysis. The weight ratios of EC and IC were 1:1 (T1), 2:1 (T2), and 1:2 (T3). T1 was the general optimum scheme, with values of the design parameters as follows: building orientation, 0°; the insulation thickness of roof and east, south, west, and north wall of 0.13 m, 0.03 m, 0.03 m, 0.08 m, and 0.06 m, respectively, with insulation material of EPS board; OL, EL, and TA of sunvisor of 0.8 m, 0.3 m, and 90°, respectively; Window type, "single Low-e clear 6 mm"; width of south and north windows, 1.9 m and 1.5 m; height of first and second floor south windows, 1.5 m and 1.7 m; and height of first and second floor north windows, 2.0 m and 1.7 m. When the weighted values (F) of several schemes are very similar, the optimal scheme can be determined according to the design parameters that having differences between the different schemes. In particular, focusing on the synthetic parameters, which not only affect the energy consumption and cost, but also have an impact on building style or layout.

In this paper, a multi-objective optimization method for determining the values of architectural design parameters was introduced, which can be applied to the design of rural house in Hanzhong region, an area characterized by hot summer and cold winter. The presented results can assist designers to solve the contradiction of multiple objectives at the scheme design stage, playing a beneficial role in reducing building energy consumption and initial investment cost. Furthermore, in follow-up research, the type and number of optimization objectives or design variables can also be adjusted according to the actual requirements such as the thermal comfort, daylighting performance etc., and active design measures may be extended in design variables in order to obtain a design scheme with better comprehensive performance.

Author Contributions: Conceptualization, T.S.; methodology, T.S. and W.Z.; software, T.S.; validation, T.S. and Z.C.; formal analysis, T.S., W.Z. and Z.C.; investigation, T.S. and W.Z.; resources, T.S.; data curation, T.S.; writing—original draft preparation, T.S., W.Z. and Z.C.; writing—review and editing, T.S., W.Z. and Z.C.; visualization, T.S.; supervision, T.S.; project administration, T.S.; funding acquisition, T.S. All authors have read and agreed to the published version of the manuscript.

Funding: This research was funded by the Humanities and Social Sciences Project of Ministry of Education of the PRC, grant number 20YJC760081; the Science and Technology Program of Ministry of Housing and Urban–Rural Development of the PRC, grant number 2019-K-126; and the China Postdoctoral Science Foundation, grant number 2019M663820.

Data Availability Statement: The data that support the findings of this study are available from the corresponding author, T.S., upon reasonable request.

Conflicts of Interest: The authors declare no conflict of interest.

References

1. Sterner, T. Fuel taxes: An important instrument for climate policy. *Energy Policy* **2007**, *35*, 3194–3202. [[CrossRef](#)]
2. Ministry of Housing and Urban-Rural Development of PRC. *Technical Standard for Nearly Zero Energy Buildings (GB/T 51350-2019)*; China Architecture Industry Press: Beijing, China, 2019.
3. Zou, Y.; Song, B.; Liu, J. An interpretation of the national standards for energy efficiency design of rural residential buildings. *Heat. Vent. Air Cond.* **2013**, *43*, 77–81.
4. Shao, T.; Zheng, W.X.; Jin, H. Analysis of Indoor Thermal Environment and Passive Energy Saving Optimization Design of Rural Dwellings in Zhalantun Area, Inner Mongolia, China. *Sustainability* **2020**, *12*, 1103. [[CrossRef](#)]
5. Building Energy Efficiency Research Center, Tsinghua University. *2021 Annual Report on China Building Energy Efficiency*; China Architecture & Building Press: Beijing, China, 2021.
6. Ministry of Housing and Urban-Rural Development of PRC. *The 13th Five-Year Plan of Building Energy Conservation and Green Building Development*; Ministry of Housing and Urban-Rural Development of PRC: Beijing, China, 2017.
7. Ma, C.; Liu, Y.; Wang, D. Analysis of thermal performance and energy saving strategy of rural residential buildings in Northwest China. *J. Xi'an Univ. Arch. Technol* **2015**, *47*, 427–432.
8. Chen, X.; Yang, H.; Lu, L. A comprehensive review on passive design approaches in green building rating tools. *Renew. Sustain. Energy Rev.* **2015**, *50*, 1425–1436. [[CrossRef](#)]
9. ECGB Editorial Department. Regional Green Building in the Background of Urban-Rural Integration: Interview with Academician Liu Jiaping, Professor of College of Architecture, Xi'an University of Architecture & Technology. *Eco-City Green Build.* **2014**, *1*, 16–17.
10. Zhu, X.R.; Liu, J.P.; Yang, L.; Hu, R.R. Energy performance of a new Yaodong dwelling, in the Loess Plateau of China. *Energy Build.* **2014**, *70*, 159–166. [[CrossRef](#)]
11. Yang, W.J.; Gao, Q.; Xu, B.; Yin, S.S. Inheriting and Updating the Technology of Low Energy Consumption Used in Waterside Vernacular Dwellings in the Lower Yangtze Basin. *Archit. J.* **2015**, *1*, 66–69.
12. Yang, W.J.; Xu, B.; Chang, L. Research on the Ecological Design Strategy of Rural Housing in Qinghai. *Eco-City Green Build.* **2015**, *Z1*, 112–119.
13. Zhou, T.J.; Liu, H.J. A Study on the Application of Low-tech Energy-saving Strategies in the New Rural Residence in Sichuan Province—Examined by the Residential Design of the No.2 Settlements in Nanlin Village, Xiwai Township, Guanghan City. *Hum. Settl. Forum West China* **2014**, *3*, 32–37.
14. He, Q.; Gao, H.Q.; Liu, D.L.; Zhu, X.R. Study on Energy Saving Optimization of Traditional Houses in Lhasa. *Archit. Cult.* **2019**, *180*, 243–245.
15. Hao, S.M.; Song, Y.H.; Li, J.J.; Zhu, N. Field Study on Indoor Thermal and Luminous Environment in Winter of Vernacular Houses in Northern Hebei Province of China. *J. Harbin Inst. Technol.* **2014**, *21*, 77–83.
16. Sun, H.J.; Leng, M.J. Analysis on building energy performance of Tibetan traditional dwelling in cold rural area of Gannan. *Energy Build.* **2015**, *96*, 251–260. [[CrossRef](#)]
17. Liu, S.; Huang, C.H. Analysis of the Thermal Environment and Energy-Saving Retrofitting of a Traditional Dwelling in Western Hunan. *Build. Sci.* **2016**, *6*, 27–32.
18. Xu, G.Q.; Jin, H.; Kang, J. Experimental Study on the Indoor Thermo-Hygrometric Conditions of the Mongolian Yurt. *Sustainability* **2019**, *11*, 687.
19. Jin, H.; Ling, W. Low Energy Consumption, Low-tech and Low Cost: Study on the Design for Rural Energy-saving Housing in Cold Region. *Archit. J.* **2010**, *8*, 14–16.
20. Zhang, X.Y.; Jin, H. Strategies of function improvement on existing rural housing in severe cold and cold regions. *J. Harbin Inst. Technol.* **2011**, *18*, 117–121.
21. Li, G.; Feng, G.H.; Wang, L.; Wang, Q.; Li, Z. Energy consumption simulation and analysis on energy saving reconstruction of rural house in China extreme cold areas. *J. Shenyang Jianzhu Univ.* **2012**, *28*, 884–890.
22. Li, J.; Zou, Y.; Liu, J. Study on Building Envelope Optimization Parameters and Energy-saving Rate of Rural Residential Buildings in Severe Cold and Cold Zones. *Build. Sci.* **2012**, *28*, 6–9.
23. Lv, S.L.; Wang, R.; Zheng, S.Q. Passive Optimization Design Based on Particle Swarm Optimization in Rural Buildings of the Hot Summer and Warm Winter Zone of China. *Sustainability* **2017**, *9*, 2288.
24. Gossard, D.; Lartigue, B.; Thellier, F. Multi-objective optimization of a building envelope for thermal performance using Genetic Algorithms and Artificial Neural Network. *Energy Build.* **2013**, *67*, 253–260. [[CrossRef](#)]

25. Ascione, F.; Bianco, N.; Stasio, C.D.; Mauro, G.M.; Vanoli, G.P. A new methodology for cost-optimal analysis by means of the multi-objective optimization of building energy performance. *Energy Build.* **2015**, *88*, 78–90. [[CrossRef](#)]
26. Delgarm, N.; Sajadi, B.; Delgarm, S.; Kowsary, F. A novel approach for the simulation-based optimization of the buildings energy consumption using NSGA-II: Case study in Iran. *Energy Build.* **2016**, *127*, 552–560. [[CrossRef](#)]
27. Bre, F.; Roman, N.; Fachinottia, V.D. An efficient metamodel-based method to carry out multi-objective building performance optimizations. *Energy Build.* **2020**, *206*, 109576. [[CrossRef](#)]
28. Harkouss, F.; Fardoun, F.; Biwole, P.H. Multi-Objective Optimization Methodology for Net Zero Energy Buildings. *J. Build. Eng.* **2018**, *16*, 57–71. [[CrossRef](#)]
29. Yu, Z.Y.; Lu, F.; Zou, Y.; Xu, W.; Sun, D.Y.; Liu, C.P. A Simulation-based Multi-objective Optimization Approach for Design of Nearly Zero Energy Buildings. *Build. Sci.* **2019**, *35*, 8–15.
30. Zhu, L.; Wang, B.H.; Sun, Y. Multi-objective optimization for energy consumption, daylighting and thermal comfort performance of rural tourism buildings in north China. *Build. Environ.* **2020**, *176*, 106841. [[CrossRef](#)]
31. Hong, T.; Kim, J.; Lee, M. A multi-objective optimization model for determining the building design and occupant behaviors based on energy, economic, and environmental performance. *Energy* **2019**, *174*, 823–834. [[CrossRef](#)]
32. Xiao, Q.B. Research on Energy Saving Optimization of Exterior Wall and Roof Structure of Existing Rural Houses in the Ningqiang Region of South Shaanxi Province. Master's Thesis, Northwestern Polytechnical University, Xi'an, China, 2019.
33. Ministry of Housing and Urban-Rural Development of PRC. *Design Standard for Energy Efficiency of Rural Residential Buildings (GB/T 50824)*; Chinese Architecture Industry Press: Beijing, China, 2013.
34. Ministry of Housing and Urban-Rural Development of PRC. *Code for Thermal Design of Civil Building. Chinese Architecture (GB 50176-2016)*; Chinese Architecture Industry Press: Beijing, China, 2016.
35. Ministry of Housing and Urban-Rural Development of PRC. *Design Standard for Energy Efficiency of Residential Buildings in Hot Summer and Cold Winter Zone (JGJ 134-2010)*; Chinese Architecture Industry Press: Beijing, China, 2010.
36. ASHRAE. *ANSI/ASHRAE Standard 140-2007, Standard Method of Test for the Evaluation of Building Energy Analysis Computer Programs*; ASHRAE: Atlanta, GA, USA, 2007.
37. Krzysztof, G.; Joanna, F.G. Multi-Objective Optimization of the Envelope of Building with Natural Ventilation. *Energies* **2018**, *11*, 1383.
38. Palonen, M.; Hamdy, M.; Hasan, A. MOBO A New Software for Multi-Objective Building Performance Optimization. In Proceedings of the 13th Conference of International Building Performance Simulation Association, Chambéry, France, 26–28 August 2013.
39. Evins, R. A review of computational optimization methods applied to sustainable building design. *Renew. Sustain. Energy Rev.* **2013**, *22*, 230–245. [[CrossRef](#)]
40. Deb, K.; Pratap, A.; Agarwal, S. A fast and elitist multi-objective genetic algorithm: NSGA-II. *IEEE Trans. Evol. Comput.* **2002**, *6*, 182–197. [[CrossRef](#)]
41. Delgarm, N.; Sajadi, B.; Delgarm, S. Multi-objective optimization of building energy performance and indoor thermal comfort: A new method using artificial bee colony (ABC). *Energy Build.* **2016**, *131*, 42–53. [[CrossRef](#)]
42. Yu, W.; Li, B.Z.; Jia, H.Y.; Zhang, M.; Wang, D. Application of multi-objective genetic algorithm to optimize energy efficiency and thermal comfort in building design. *Energy Build.* **2015**, *88*, 135–143. [[CrossRef](#)]
43. Asadi, E.; Silva, M.G.D.; Antunes, C.H.; Dias, L.; Glicksman, L. Multi-objective optimization for building retrofit: A model using genetic algorithm and artificial neural network and an application. *Energy Build.* **2014**, *81*, 444–456. [[CrossRef](#)]
44. Yusoff, Y.; Ngadiman, M.S.; Zain, A.M. Overview of NSGA-II for Optimizing Machining Process Parameters. *Procedia Eng.* **2011**, *15*, 3978–3983. [[CrossRef](#)]
45. Si, B.H.; Wang, J.G.; Yao, X.Y.; Shi, X.; Jin, X.; Zhou, X. Multi-objective optimization design of a complex building based on an artificial neural network and performance evaluation of algorithms. *Adv. Eng. Inform.* **2019**, *40*, 93–109. [[CrossRef](#)]
46. Zhao, H.; Jin, H. Research on the local optimum eco-technologies of rural housing in the chill region of China. *J. Harbin Inst. Technol.* **2007**, *39*, 235–237.